POLITECNICO DI TORINO

Master's Degree in Mechatronic Engineering

Master's Degree Thesis

Optimization of fuel consumption of a Hybrid Electric Vehicle with Adaptive Cruise Control

Supervisors

Prof. Andrea TONOLI

Dr. Stefano FAVELLI

Dr. Eugenio TRAMACERE

Eng. Andrea DELMASTRO

Candidate

Nadia EL AMRANI

DECEMBER 2023

Summary

One of the major goals of the automotive industry in recent years has been the improvement of the energy efficiency of vehicles, due to the restrictions on emissions and the increasing energy costs. The EU is aiming to achieve by 2050 a reduction of transportation greenhouse gas emissions of 90% compared to 1990. To reach this objective, electrification and automation are becoming the main trends in the automotive field. The growth of autonomous vehicles is important not only for the reduction of car accidents, but also for the improvement of fuel economy. Fuel consumption strictly depends on driving behavior, therefore technologies for autonomous vehicles such as Advanced Driver Assistance System (ADAS) are used to adjust the driving style enhancing eco-driving. ADAS technologies are a set of features that reduce human duties in driving, improving safety, comfort and emissions. In particular, high acceleration and deceleration values correspond to high torque requests, which can be satisfied by the system at the expense of emissions. To overcome this problem, Adaptive Cruise Control (ACC) can be exploited. ACC is an ADAS application that manages and optimizes the acceleration values of the system, based on the velocity profile of a preceding vehicle (called "lead vehicle"). A car equipped with ACC can work in two modes: car-following, in which the vehicle follows the preceding one, and cruising, in which the vehicle travels at a set speed. The car-following mode is the most significant for eco-ACC employment since the driving profile of the lead car can be used for prediction and optimization of the behavior of the ego car.
This thesis work investigates the benefits of using Eco-Adaptive Cruise Control in a mild-hybrid P1 IVECO Daily vehicle. In addition to the

verification of car-following performances, the work focuses on studying the potential for fuel consumption reduction and energy efficiency enhancement.

In this thesis Eco-ACC was integrated with a forward vehicle model developed in Matlab/Simulink. In literature many examples of eco-ACC algorithms are reported. The one exploited in this work evaluates the acceleration command based on a minimization problem. The controller receives as input the relative speed and distance from the lead vehicle, obtained through the use of radars and camera sensors, and finds the optimal acceleration command to satisfy two main objectives: travel at a set velocity when the lead vehicle is far enough, or slow down when the safety distance is not respected anymore. The car-following performance depends on some tuning parameters which are the desired time gap and the error gains on the relative distance, relative speed and set speed. The time gap is defined as the time that passes between the lead and ego vehicles as they go through the same point. The set speed and the minimum safety distance are fixed parameters. Since the objective is to use the eco-ACC exploiting the car-following mode, the set speed has been put very high (50 m/s) and the relative error gain very low, to minimize the effect of this constraint. In this way, the ego vehicle can follow the lead car even at high speeds. To test the system, it was supposed that the lead car followed the speed profiles of standard driving cycles, used by automotive organizations for the verification of emissions. The considered driving cycles were the WLTC and RDE, developed by the United Nations Economic Commission for Europe, and the FTP75 and US06 developed by the Environmental Protection Agency of the United States of America. Firstly, the tests were performed to verify the car-following performances. It was required that the speed of the ego car was in the 10% range of the lead car velocity. In addition, the relative distance needed to be higher than the minimum safety distance, but low enough so that the lead car could be in the view range of the sensors. This upper threshold was decided based on the scenario, so for speeds typical of urban roads the limit was 50 meters, 150 for suburban and 250 for motorways. The time gap

was tuned to satisfy these requirements. The minimum safety distance was fixed at 10 meters for all scenarios. In addition, the gains were tuned to obtain a stable acceleration reference command as the output of the controller. In fact, an aggressive controller led to a saturated and unstable command, because it could not achieve the requested performances. After the verification of the car-following behavior, it was possible to evaluate the benefit of the controller in terms of fuel economy and comfort. To analyze the advantages of eco-ACC, the results were compared to the ones obtained from the simulations of the vehicle model not equipped with ACC, traveling using the same driving cycle as reference speed. The simulations showed that for low-speed scenarios with low values of acceleration, a time gap of 3 seconds resulted in good performances. The fuel consumption reduction was between 9% and 14% for urban scenarios and between 5% and 10 % for rural scenarios, with time gap increased to 4 seconds. Analyzing the BSFC map of the ICE, it was possible to notice that the model equipped with eco-ACC worked with lower torques and therefore higher efficiency, and the working points area decreased with the increasing time gap. For highways scenarios, the results did not show any significant improvement in fuel consumption. The BSFC map showed that the system was working with high torques, and the eco-ACC could not bring any optimization in the torque management logic.
Then, the controller was modified introducing a function to obtain an adaptive time gap depending on the actual velocity of the vehicle. This function calculates the moving average of the last n values of the actual speed and compares it to velocity thresholds obtained while tuning the constant time gap controller. The time gap of the controller is then changed based on the comparison. This new controller was tested on the RDE complete, which is a driving cycle representative of all the different scenarios. It was possible to observe that thanks to this new function, the velocity speed was kept in the 10% range of the lead velocity and the relative distance was in the desired interval through the entire cycle. Moreover, this control logic introduces an additional improvement in fuel consumption, with respect to the constant time gap ACC.

Acknowledgements

Ai miei genitori, a voi devo tutto. Per aver sempre creduto in me e avermi sostenuta in tutte le mie scelte. Per avermi insegnato a essere forte in ogni situazione e a non arrendermi davanti agli ostacoli. Per i vostri sacrifici e il vostro amore.
A mio fratello Dawid, per avermi supportata e sopportata in tutti questi anni, aiutandomi ad affrontare la vita con leggerezza e a ridere di fronte alle difficoltà. A mio fratello Rachid, che mi ha insegnato a osservare il mondo con curiosità fin da quando ero piccola.
A Daniela, per esserci stata in ogni istante, per ogni risata e ogni pianto, per avercela fatta insieme come sempre. Sono stati cinque anni difficili, ma averli affrontati con te ha reso tutto più bello.
A Elena, per esser capace di farmi vedere la vita da una prospettiva migliore, calmando inconsapevolmente le mie ansie. Ovunque saremo, per me sarai per sempre casa.
A tutti i miei amici, per essermi stati a fianco e aver alleggerito anche le giornate più difficili.
Alla mia famiglia, che dal Marocco ha sempre fatto il tifo per me, coprendo la distanza con amore incommensurabile.

Al professor Tonoli, per avermi dato la possibilità di partecipare a questo progetto.
A Stefano e a Eugenio, senza cui questo lavoro non sarebbe stato possibile. Grazie per avermi guidata e aiutata con dedizione e pazienza.
La passione che mettete nel vostro lavoro sarà sempre di esempio per me.

Table of Contents

List of Tables x

List of Figures xii

Acronyms xvi

1 Introduction 1
- 1.1 Background . . . 1
  - 1.1.1 Electrification . . . 2
  - 1.1.2 Automation . . . 3
- 1.2 Project overview . . . 5
- 1.3 Thesis outline . . . 5

2 Theoretical background 7
- 2.1 Hybrid Electric Vehicles . . . 7
  - 2.1.1 HEVs Classification . . . 7
  - 2.1.2 HEVs Classification based on architecture . . . 8
  - 2.1.3 HEVs Classification based on hybridization . . . 10
- 2.2 Energy Management System . . . 12
  - 2.2.1 Equivalent Consumption Minimization Strategy 14
  - 2.2.2 Adaptive ECMS . . . 18
- 2.3 Advanced Driver Assistance System . . . 19
  - 2.3.1 ADAS regulation in Europe . . . 21
- 2.4 Verification and validation of ADAS . . . 21
  - 2.4.1 In-the-loop simulations . . . 22
  - 2.4.2 European New Car Assessment Programme . . 24

2.5 Testing methodology: scenarios 25
2.6 Case of study: Adaptive Cruise Control 27
2.6.1 ACC strategies to minimize fuel consumption (Eco-ACC): State of Art 28

3 Model and strategy 32
3.1 Vehicle model overview 32
3.1.1 Plant 34
3.1.2 Energy analysis of the powertrain 35
3.1.3 Controller 39
3.1.4 Efficiency maps 43
3.2 ACC controller 45
3.2.1 Starting model: Mathworks ACC with Sensor Fusion 45
3.2.2 Integration in the IVECO Daily model 47
3.2.3 Classical ACC 48
3.3 Tested scenarios 50
3.3.1 Driving cycles 50

4 Simulations and results 57
4.1 Simulations strategy 57
4.2 Simulations on the system equipped with Classical ACC 59
4.3 Integration and test of adaptive-time gap function in Classical ACC 78

5 Conclusion 83
5.1 Future works 84

Bibliography 86

List of Tables

2.1 HEV classification based on hybridization degree [8] . . 11
2.2 Estimated consumption benefits for the different HEV . 12

3.1 Values of dissipation forces coefficients in the model . . 36
3.2 Battery specifications 37
3.3 PID parameters 40
3.4 NEDC parameters 52
3.5 WLTC parameters 53
3.6 FTP-75 parameters 55
3.7 US06 parameters 56

4.1 Safety distance thresholds 58
4.2 Fixed parameters 59
4.3 Gains values 59
4.4 Car-following parameters in WLTC cycle 61
4.5 Fuel consumption in WLTC cycle 63
4.6 Car-following parameters in FTP75 cycle 64
4.7 Fuel consumption in FTP75 cycle 65
4.8 Car-following parameters in RDE urban cycle 67
4.9 Fuel consumption in RDE urban cycle 69
4.10 Car-following parameters in RDE rural cycle 70
4.11 Fuel consumption in RDE rural cycle 72
4.12 Car-following parameters in RDE motorway cycle . . . 74
4.13 Fuel consumption in RDE motorway cycle 75
4.14 Car-following parameters in US06 cycle 77
4.15 Fuel consumption in US06 cycle 77

4.16 Time gap values for the different driving cycles 79
4.17 Thresholds for adaptive time gap function 80
4.18 Fuel consumption improvement with respect to lead vehicle in RDE complete cycle 81

5.1 Fuel saving for each cycle with constant time gap ACC 84

List of Figures

1.1 Evolution of CO2 emissions in the EU for each sector (1990-2019) [2] 2
1.2 Electric cars sales (2016 - 2023) 3
1.3 SAE automation levels 4

2.1 Series HEV configuration [7] 8
2.2 Parallel HEV configuration [7] 9
2.3 Possible positions of the EM in the parallel configuration 10
2.4 Combined HEV configuration [7] 11
2.5 Control architecture in a HEV [10] 13
2.6 Energy path in the discharging phase (a) and in the charging phase (b) for a parallel HEV. [10] 15
2.7 Penalty factor in function of battery SOC and exponent a [10] 17
2.8 Dependency of SOC variation and fuel consumption with respect to s_{charge} and $s_{discharge}$ factors [10] 17
2.9 ADAS equipment on a vehicle 20
2.10 V-Shape diagram for the design and validation phases in the development of automotive safety-critical systems 22
2.11 Vehicle under test in VeHIL [17] 24
2.12 Cut-in scenario from NCAP tests [20] 26
2.13 Cut-out scenario. In blue the ego vehicle and in red the lead vehicle [22] 26
2.14 Approach of a stopped vehicle. In blue the ego vehicle and in red the lead vehicle [22] 27
2.15 ACC hierarchical structure 28

2.16 Scenario of the control strategy exploited in [24] 30

3.1 Forward scheme (on top) and backward scheme (on bottom) [30] 33
3.2 Forward model of the vehicle on Matlab/Simulink . . . 33
3.3 Plant of the model 34
3.4 Powertrain model 35
3.5 Energy losses related to speed 37
3.6 Battery current profile. The black lines indicate the current limit due to C-rate and power electronics restrictions. 39
3.7 Controller model 39
3.8 Driver PI controller 40
3.9 Charge Depleting and Charge Sustaining modes of a battery. [31] 42
3.10 Relay block for equivalence factor evaluation 42
3.11 BSFC map 44
3.12 EM efficiency map 44
3.13 ACC with Sensor Fusion Mathworks model testbench . 46
3.14 ACC with Sensor Fusion Mathworks model 46
3.15 High-level controller with ACC 47
3.16 High-level controller with ACC and scenario reader. . . 48
3.17 Time gap and headway graphic representation [33] . . . 49
3.18 Classical ACC Simulink model 50
3.19 NEDC speed profile 51
3.20 WLTP cycle 53
3.21 RDE specifications 54
3.22 FTP-75 cycle [36] 55
3.23 US06 cycle [37] 56

4.1 Simulation strategy 57
4.2 Speed profile for WLTC cycle, time gap = 1.5 s 60
4.3 Speed profile for WLTC cycle, time gap = 3 s 60
4.4 Acceleration and speed profile in WLTC cycle, time gap = 1.5 s 61
4.5 Acceleration and speed profile in WLTC cycle, time gap = 3 s 62

4.6 Relative distances in WLTC cycle 62
4.7 BSFC map in WLTC cycle 63
4.8 Acceleration and speed profile in FTP75 cycle, time gap = 3 s 64
4.9 BSFC map in FTP75 cycle 65
4.10 Speed profile for RDE urban cycle, time gap = 1.5 s . . 66
4.11 Speed profile for RDE urban cycle, time gap = 3 s . . . 66
4.12 Relative distance for RDE urban cycle 67
4.13 Acceleration and speed profile for RDE urban cycle, time gap = 1.5 s 68
4.14 Acceleration and speed profile for RDE urban cycle, time gap = 3 s 68
4.15 BSFC map in RDE urban cycle 69
4.16 Speed profile for RDE rural cycle, time gap = 4 s . . . 70
4.17 Relative distance for RDE rural cycle 71
4.18 Acceleration and speed profile for RDE rural cycle . . . 71
4.19 BSFC map in RDE rural cycle 72
4.20 Velocity and relative distance in RDE motorway with time gap 5 seconds 73
4.21 Velocity and relative distance in RDE motorway with time gap 8 seconds 73
4.22 Acceleration profile in RDE motorway with time gap 8 seconds 74
4.23 BSFC map in RDE motorway cycle 75
4.24 Velocity and acceleration in US06 with time gap 8 seconds 76
4.25 Relative distance in US06 with time gap 8 seconds . . . 77
4.26 BSFC map in US06 cycle 78
4.27 Velocity and time gap on RDE complete 80
4.28 Velocity on RDE complete - high speeds 81
4.29 Relative distance on RDE complete 82

Acronyms

ADAS

Advanced Driver Assistance Systems

ACC

Adaptive Cruise Control

AEB

Autonomous Emergency Braking

BSFC

Brake Specific Fuel Consumption

CD

Charge Depleting

CS

Charge Sustaining

DoH

Degree of Hybridization

ECMS

Equivalent Consumption Minimization Strategy

EM

Electric Motor

EMS

Energy Management System

FL

Fuzzy Logic

GVT

Global Vehicle Target

HEV

Hybrid Electric Vehicle

HIL

Hardware-In-the-Loop

ICE

Internal Combustion Engine

LIDAR

Light Detection And Ranging

LQR

Linear Quadratic Regulator

MIL

Model-In-the-Loop

MPC

Model Predictive Control

PID

Proportional Integrative Derivative controller

PMR

Power-to-Mass Ratio

SIL

Software-In-the-Loop

SOC

State Of Charge

TTC

Time To Collision

VeHIL

Vehicle-Harware-in-the-loop

VUT

Vehicle Under Test

Chapter 1

Introduction

1.1 Background

The automotive field has a major impact on global pollution. According to the report of the European Environment Agency, the transportation sector was responsible for almost 25% of the total greenhouse gas emissions in the European Union in 2019, with road transportation contributing to 72% of it [1]. Greenhouse gases include CO_2 and NOx. The increase of these elements in the air has an impact not only on climate change (due to the greenhouse effect that contributes to the increase of global temperatures), but also on human health, leading to respiratory diseases. Therefore, the minimization of vehicles emissions has become a key point for governments and automotive industries. The EU is aiming to achieve by 2050 a reduction of transportation greenhouse gas emissions of 90% compared to 1990.

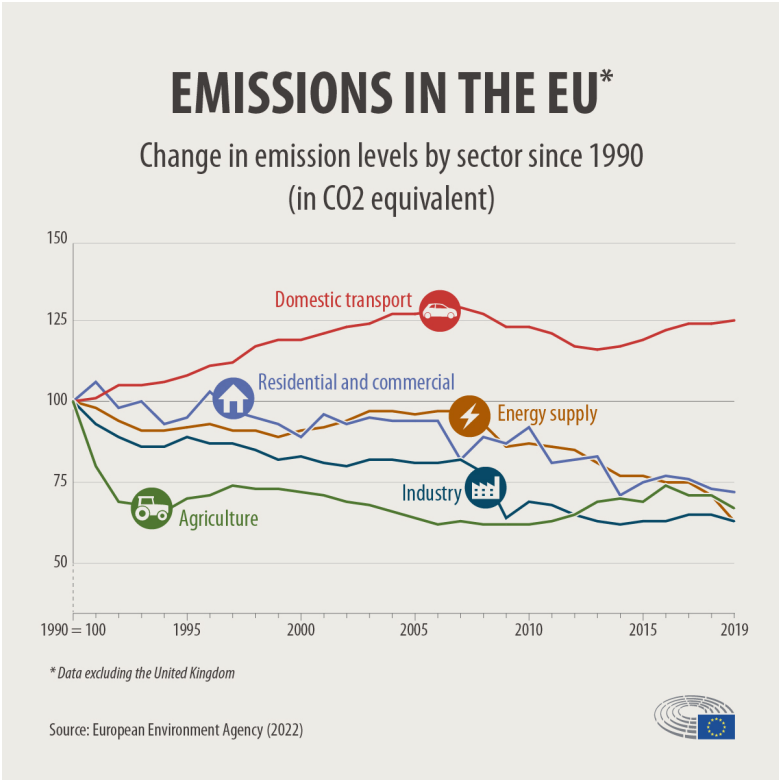

Figure 1.1: Evolution of CO2 emissions in the EU for each sector (1990-2019) [2]

1.1.1 Electrification

Electrification has a big role in the minimization of vehicles emissions. The term electrification refers to the substitution of thermal power (obtained with fuel) with electric power. This can happen in the form of pure electric vehicles or in hybrid electric vehicles, where a combustion engine is still present.
According to the "Electric vehicles from life cycle and circular economy perspectives" report of the European Environment Agency [3], electric vehicles' greenhouse gas emissions on their entire life cycle are up to 30% lower with respect to petrol and diesel cars. Considering that the EU is also going through a decarbonization of the energy mix, this percentage is predicted to reach 73% by 2050 [4].
The electric cars market has seen an important growth of sales, from

4% of total car sales in 2020 to 14% in 2022. This is due not only to government incentives for electric vehicles purchase, but also to the constantly increasing fuel costs. In addition, electric vehicles also reduce noise pollution and therefore contribute to a better environmental quality.

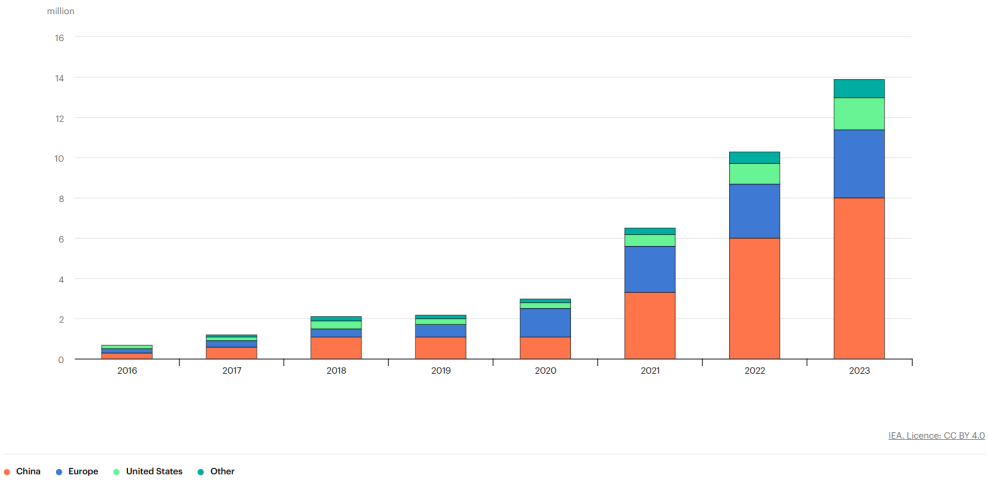

Figure 1.2: Electric cars sales (2016 - 2023)

1.1.2 Automation

The growth of autonomous vehicles is an important field in the automotive industry especially for its great impact on the decreasing of car accidents.
In fact, a survey conducted by the National Highway Traffic Safety Administration (NHTSA) demonstrated that 94% of car crashes are due to human errors. [5]
Therefore, increasing the automation levels means reducing the driver's responsibility, obtaining an optimized driving behaviour and consequently also reducing accidents.
The Society of Automotive Engineers (SAE) has defined a scale of six levels of automation, specified in Figure 1.3. These guidelines have been updated in 2021 and are adopted by the United Nations.[6]

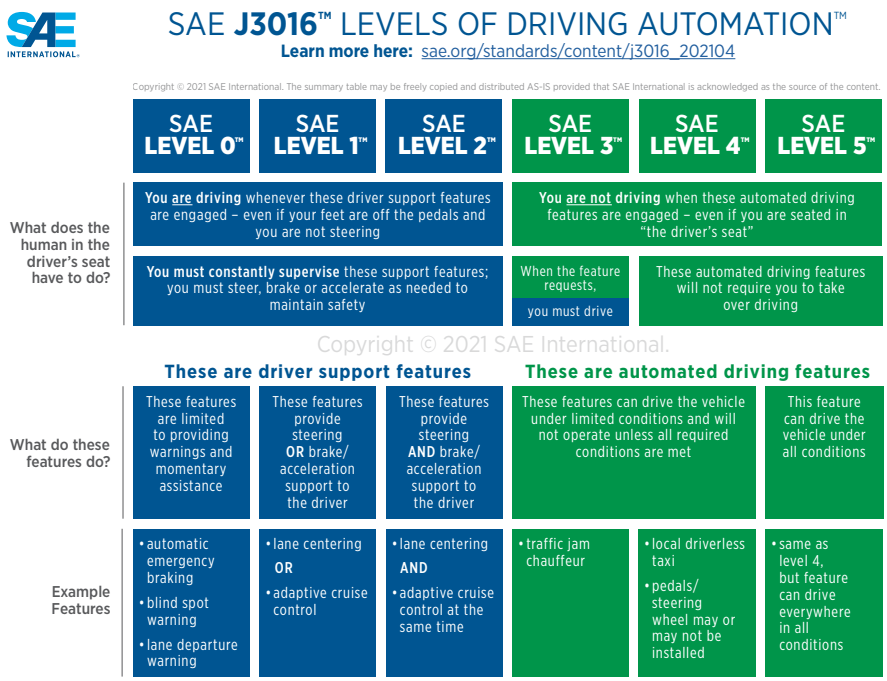

Figure 1.3: SAE automation levels

The automation levels are classified from Level 0 (no automation) to Level 6 (full automation), based on the duties of the driver.
Levels 0 to 2 require the driver to have full attention on the road, but the vehicle is equipped with some support features that assist him during driving. In levels 3 to 5 the driver is not required to drive, except for some situations that may be requested by the automated features in Level 3.
The majority of vehicles that are on the market right now only reach Level 2 automation, such as the Tesla Autopilot.
For what concerns Level 3, Mercedes-Benz EQS and Class S equipped with Drivepilot have been approved on the market in Germany and in some states in the USA. Under specific conditions, the drivers of these vehicles are allowed to legally travel without watching the road or touching the commands at all.
Level 4 vehicles have been successfully tested on the road but they

have not been approved for consumer use anywhere in the world yet. Some Level 4 vehicle for taxi use are approved, such as Waymo One in California.
Level 5 has not been reached yet, and it is a great challenge that some experts believe we will never get to. The main issues about a complete autonomous driving experience are mainly due to external factors such as roads, culture and environmental conditions.

1.2 Project overview

This thesis work is part of the "AutoEco" project funded by Pi.Te.F. (Piattaforma Tencologica di Filiera) of the Piedmont region in collaboration with Politecnico di Torino, Dayco Europe S.r.l, Podium Advanced Technologies and other companies. The aim of this project is the hybridization and automation of a light-duty hybrid electric vehicle, in the optic of reduction of fuel consumption and increase of energy efficiency.

1.3 Thesis outline

This thesis work is divided into five chapters.

1. *Introduction*: this chapter is a contextualization of the work, identifying the motivations and the alignment with current automotive trends for electrification and automation.

2. *Theoretical background*: an overview on hybrid electrical vehicles and their energy management systems is presented, to better comprehend the starting model of the project. ADAS technologies are then introduced, along with their verification and validation methods. An overview of Adaptive Cruise Control strategies for ecological driving is then presented, as the case of study of this thesis work.

3. *Model and strategy*: this section begins with the analysis of the vehicle model, with emphasis on the energy aspects. Then the Adaptive Cruise Control strategy adopted is presented, and the introduction of this control system in the complete model is explained, along with the driving scenarios used for testing.

4. *Simulations and results*: the objective of this chapter is to present the simulations of the complete system and the obtained results, with charts and tables. The results are analyzed and a new possible algorithm is formulated to overcome the flaws of the initially adopted control strategy.

5. *Conclusion*: the last chapter is dedicated to an overview of the main points of this thesis work, highlighting possible future developments.

Chapter 2

Theoretical background

2.1 Hybrid Electric Vehicles

Hybrid Electric Vehicles (HEV) are characterized by the presence of two power sources: an internal combustion engine (ICE) and an electric motor (EM). The EM works both as a generator (storing energy) and as a motor (providing energy). These types of vehicles are highly appreciated because the EM can give extra power in the acceleration phase, therefore the ICE can work close to its maximum efficiency. In addition, in the braking phase, the EM can store in the battery the energy that would otherwise be dissipated.

2.1.1 HEVs Classification

HEV can have different configurations, because the components that compose the powertrain can be positioned in different ways. In addition, there are different levels of hybridization that can be achieved. Therefore, HEV can be classified depending on architecture and on hybridization.

2.1.2 HEVs Classification based on architecture

ICE and EM can be connected in different ways, therefore there are different topologies for HEVs architecture. In particular, three different categories are considered: series, parallel and series/parallel configuration.

Series configuration

In the series configuration (figure 2.1) the ICE is not directly connected to the wheels. The mechanical power produced by this motor is converted into electrical energy by a generator. This power is then transmitted to the EM which converts it again into mechanical power.

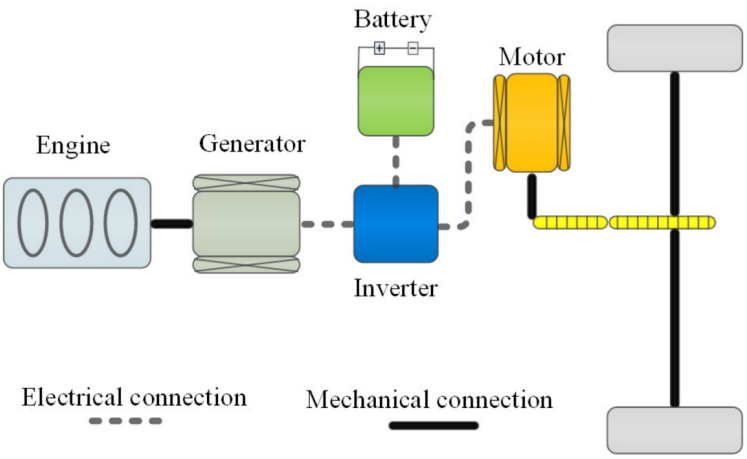

Figure 2.1: Series HEV configuration [7]

The big advantage of this configuration is that, since the ICE is not directly connected to the wheels, it can operate in its narrow most efficient rpm range even as the vehicle changes speed. Moreover, the engine can be positioned in the powertrain without constrictions.
However, the energy from the ICE has to go through several conversions, and this leads to losses that decrease the efficiency of the system.

Parallel configuration

In this configuration the power sources are two: the ICE and the EM. They are collocated in parallel and both are linked to the wheels (2.2). As a result, this configuration is flexible to switch between ICE and EM power sources. However, this system is more complex with respect to the series one, and the ICE cannot operate near its high-efficiency working points.

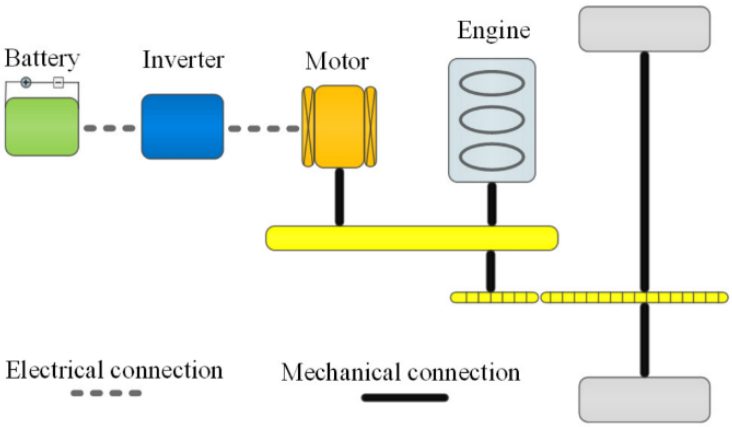

Figure 2.2: Parallel HEV configuration [7]

Parallel configuration is versatile in the positioning of the EM, offering different possible configurations:

- **P0 configuration**: The EM is positioned in the front of the ICE, connected through a belt. The two motors must have the same rotation speed and they cannot be disconnected.

- **P1 configuration**: The EM is connected directly with the crankshaft of the ICE. Also in this case the two motors must have the same rotation speed.

- **P2 configuration**: The EM is side-attached through a belt or integrated between the ICE and the transmission. A clutch is used to decouple ICE and EM.

- **P3 configuration**: The EM is connected through a gear mesh to the output of the transmission.
- **P4 configuration**: The EM is located in the axle opposite to the driving one, connected through a gear mesh.

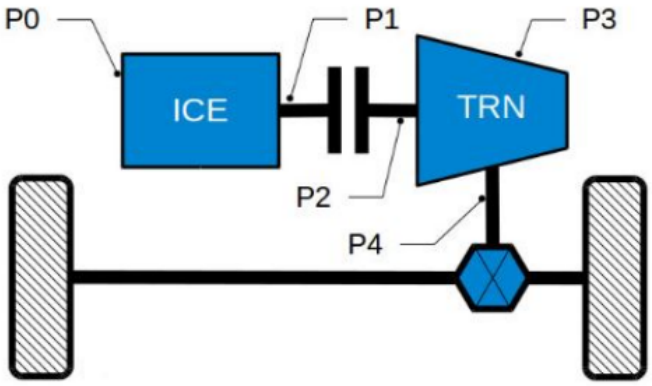

Figure 2.3: Possible positions of the EM in the parallel configuration

Combined configuration

This configuration is the most complex one (figure 2.4). Through the use of planetary gears, the different sources can be engaged or disengaged, obtaining many layouts and flexibility to switch between electric and ICE power. This power split capability allows to benefit from the advantages of both series and parallel configuration.

2.1.3 HEVs Classification based on hybridization

As mentioned before, HEV can also be classified depending on the Degree of Hybridization (DoH). The DoH is a percentage that depends on the quantity of power delivered by the ICE and the EM. It is defined as the ratio between the power delivered by the electric motor (P_{EM}) and the total power defined as the sum of electric motor and internal combustion motor ($P_{EM} + P_{ICE}$):

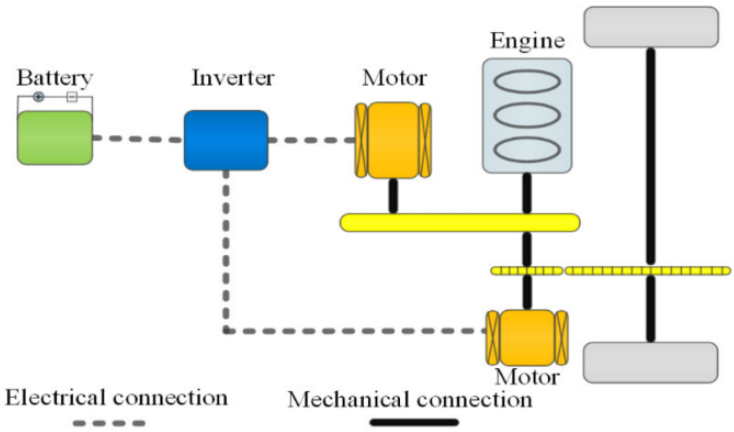

Figure 2.4: Combined HEV configuration [7]

$$DoH = \frac{P_{EM}}{P_{EM} + P_{ICE}} 100\% \tag{2.1}$$

Based on the value of this percentage, HEV can be classified as shown in the table 2.1:

Type of HEV	Deegre of Hybridization
Conventional ICE	0%
Micro-hybrid	0%<DoH< 5%
Mild-hybrid	5%<DoH<10%
Full-hybrid	10%<DoH<75%
Electric vehicle	100%

Table 2.1: HEV classification based on hybridization degree [8]

- **Conventional ICE**: This is not a hybrid vehicle since the only source of power is the ICE and there is no electric motor.
- **Micro-Hybrid**: In this configuration the Start&Stop capability of the electric motor is exploited. During idle condition the ICE can automatically shut off, saving fuel. In some cases, micro-hybrids are also characterized by the regenerative braking feature.

- **Mild-Hybrid**: This configuration exploits the same functions as micro-hybrid. In addition, the electric motor has the capability to give a power contribution in the acceleration phase and to regenerate energy in the decelerating phase.
- **Full-Hybrid**: Additionally to the features of previous categories, in full-hybrid vehicles the vehicle is able to drive in full-electric mode for limited distances.
- **Plug-in Hybrid**: This category has the same configuration as Full-hybrids, but in this case the battery can be completely discharged and then recharged by external outlets. The advantage is that this category of vehicles can drive in full-electric mode for longer distances.
- **Electric vehicle**: The ICE is not present and the vehicle is propelled only by the electric motor.

Each of these hybrid configurations has a potential fuel consumption benefit, due to the fact that the ICE is required less power. The estimated benefit is reported in the following table [9]:

Type of HEV	CO_2 estimated benefit [%]
Micro-Hybrid	5-6
Mild-Hybrid	7-12
Full-Hybrid	15-20
Plug-in Hybrid	>20

Table 2.2: Estimated consumption benefits for the different HEV

2.2 Energy Management System

The presence of different power sources in HEVs implies the need of a management system to determine which source will provide energy at each instant. This task is executed by two controllers. The low-level (or component-level) controller is responsible for the powertrain energy

sources. Using a classical feedback-control method, its job is to ensure that all the components deliver the requested power. On the other hand, the high-level (or supervisory) controller is responsible for the power splitting and energy optimization, while maintaining the battery SoC between the desired levels. This layer of the controller is the Energy Management System (EMS).
As we can see from figure 2.5 the power requested by the EMS comes directly from the speed controller, which requests the amount of power needed to follow a desired velocity profile.

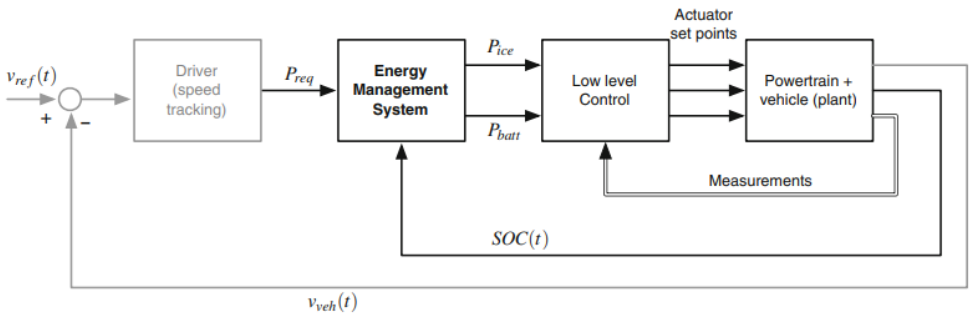

Figure 2.5: Control architecture in a HEV [10]

In literature, many energy management strategies are investigated, and they can be classified into two categories:

- **Rule-based optimization methods**: they are based on a set of rules used to determine the control value at each time, but they do not rely on explicit minimization or optimization problems. The rules are obtained from heuristics, intuition, or from mathematical models. The advantage of these methods is their effectiveness in real-time implementations.

- **Model-based optimization methods**: they rely on the global optimal solution obtained from the minimization of a cost function on a driving cycle which is fixed and known. They cannot be used for real-time implementations, but they still are a valuable approach.
  These methods can be divided into two groups:

- Numerical approaches: the global optimal solution is derived numerically taking into consideration the entire driving cycle.
- Analytical approaches: the solution is found analytically or an analytical method is derived to find the solution in a faster way than the pure numerical approach.
  Equivalent consumption minimization strategy, which will be explained in the next paragraph, belongs to this category.

2.2.1 Equivalent Consumption Minimization Strategy

Equivalent Consumption Minimization Strategy (ECMS) is a strategy used for EMS, based on the idea that the difference between the initial and final State of Charge of the battery must be negligible with respect to the total energy used in a cycle.
The State of Charge (SoC) of a battery is a percentage that indicates the level of remaining electrical charge of a battery in use.
The electrical energy used by the battery must be restored using the fuel tank or through regenerative braking. This principle relies on the definition of a cost assigned to the electrical energy. The determination of this value depends on future driving behaviour and on the driving cycle.

Given an operating point, there are two possible cases:

- Discharge case: if the battery power is positive it means that at some future point it will discharge, therefore there will be an additional fuel consumption to recharge the battery. The amount of needed fuel depends also on the capability to restore energy through regenerative braking.
- Charge case: if the battery power is negative it means that at some future point this energy will be used to contribute to the total energy requested by the powertrain. This will result in an instantaneous fuel saving.

The fundamental idea of ECMS is that electrical energy can be

associated with an equivalent value of fuel consumption, in both charge and discharge phase. This principle is illustrated in figure 2.6

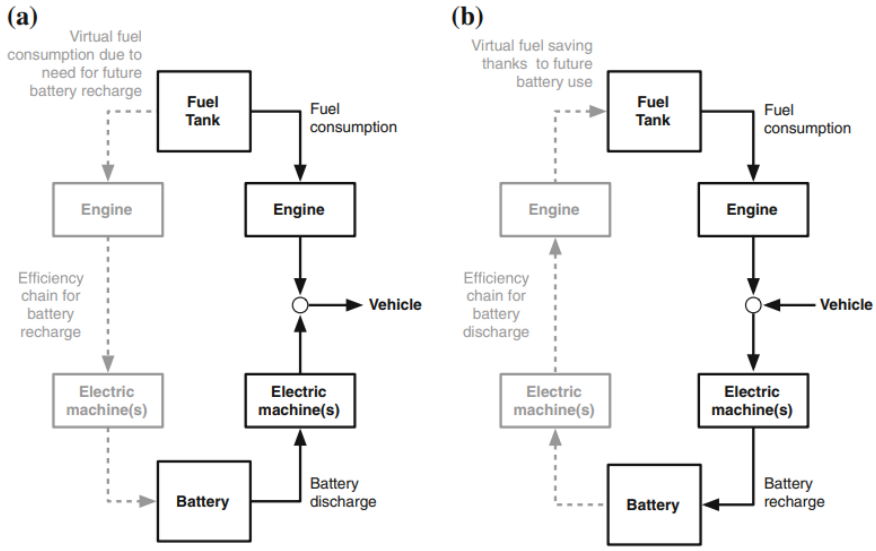

Figure 2.6: Energy path in the discharging phase (a) and in the charging phase (b) for a parallel HEV. [10]

The instantaneous equivalent fuel consumption associated to the electric energy is defined as:

$$\dot{m}_{f,eqv}(t) = \dot{m}_f(t) + \dot{m}_{ress}(t) \tag{2.2}$$

Where the real instantaneous total fuel consumption of the engine is:

$$\dot{m}_f(t) = \frac{P_{eng}(t)}{\eta_{eng}(t) Q_{lhv}} \tag{2.3}$$

Q_{lhv} is the fuel lower heating value, $\eta_{eng}(t)$ is the engine efficiency, and $P_{eng}(t)$ is the power produced by the engine when it operates at a certain efficiency.

The virtual fuel consumed by the electric machine is:

$$\dot{m}_{ress}(t) = \frac{s(t)}{Q_{lhv}} P_{batt}(t) \tag{2.4}$$

$P_{batt}(t)$ is the battery power, which can be positive or negative, depending on whether the battery is in charge or discharge mode. $s(t)$ is an equivalence factor that assigns a cost to the use of electrical power. It is a vector composed by s_{charge} and $s_{discharge}$, two terms correlated by the relationship:

$$s_{charge}(t) = (\eta_{batt})^2 s_{discharge}(t) \tag{2.5}$$

where η_{batt} is the battery charge/discharge efficiency.

The minimization problem is now reduced to a local problem (minimizing $\dot{m}_{f_{eqv}}(t)$) instead of the problem of minimizing the total cost.

$$\begin{cases} \min_{P_{batt} \in U_{P_{batt}}} \int_{t_0}^{t_f} \dot{m}_{f,eqv}(t)dt \\ \mathrm{SOC}_{min} \leq SOC \leq SOC_{max} \end{cases} \tag{2.6}$$

To assure that the SOC does not exceed the limits, a multiplicative penalty function ($p(SOC)$)is used, defined as:

$$p(SOC) = 1 - \Big(\frac{SOC(t) - SOC_{target}}{(SOC_{max} - SOC_{min})/2}\Big)^a \tag{2.7}$$

This factor takes into account the deviation of the actual SOC from the target one and compensates for it. There are three possible cases:

$$\begin{cases} \mathrm{SOC(t)} = \mathrm{SOC}_{target} \implies p(SOC) = 1 \\ \mathrm{SOC(t)} > \mathrm{SOC}_{target} \implies p(SOC) < 1 \\ \mathrm{SOC(t)} < \mathrm{SOC}_{target} \implies p(SOC) > 1 \end{cases}$$

The behaviour of $p(SOC)$ depending from the choice of the exponent a is shown in the picture 2.7:

Finally, the total instantaneous equivalent fuel equation 2.2 can be rewritten as:

$$\dot{m}_{f,eqv}(t) = \dot{m}_f(t) + \frac{s(t)}{Q_{lhv}} P_{batt}(t) p(SOC) \tag{2.8}$$

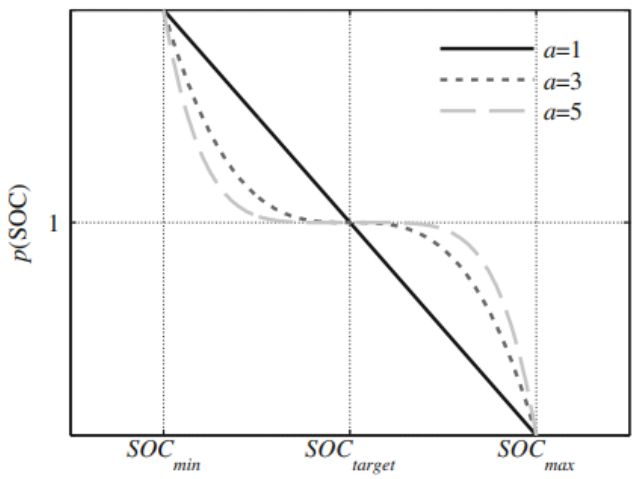

Figure 2.7: Penalty factor in function of battery SOC and exponent a [10]

The choice of the factor s is one of the main critical points of ECMS, since its definition directly affects the battery SOC and the fuel consumptions, as shown in figure 2.8.

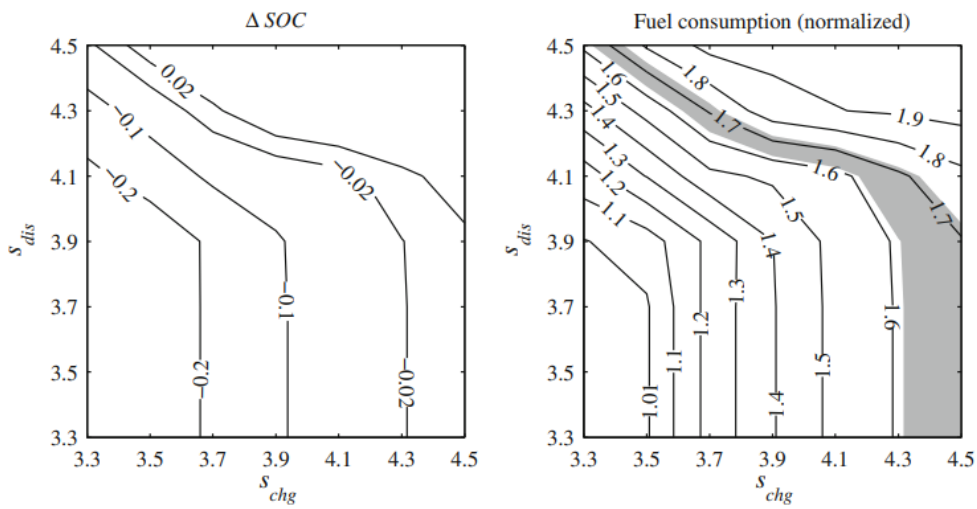

Figure 2.8: Dependency of SOC variation and fuel consumption with respect to s_{charge} and $s_{discharge}$ factors [10]

In the standard ECMS the value of the equivalence factor s is

constant, and it is calibrated offline based on the a priori knowledge of the driving cycle. There is a variant of the ECMS method, the so-called Adaptive ECMS, in which the value of s is updated online in real-time, adapting itself to the driving behaviour. This application is better described in the next paragraph.

2.2.2 Adaptive ECMS

Adaptive ECMS (A-ECMS), as mentioned in the previous section, is an online optimization strategy that constantly updates the value of the equivalence factor s, depending on the desired driving target.
There are three different categories of adaptation techniques:

1. **Adaptation based on driving cycle prediction**:
   The ECMS is integrated with a module that relates the current speed profile with the estimation of parameter s. Different approaches are adopted.
   In [11] the algorithm builds the driving mission based on information obtained by GPS data, combined with past and predicted velocity values. The equivalence factor is estimated keeping into account fuel consumption and SOC constraints. In addition, in this paper the algorithm is sped up using a single factor s for both charge and discharge phase, to reduce the problem to a one-dimensional optimization problem.
   In [12] the strategy is built up on the employment of Model Predictive Control (MPC) integrated with Intelligent Transportation Systems (ITS) information. In this way a prediction-based real-time controller is established.

2. **Adaptation based on driving pattern recognition**:
   This technique is based on the assumption that similar driving cycles correspond to similar values of s. In [13] an algorithm recognizes the driving pattern and selects the most appropriate equivalence factor from a set of precalculated values corresponding to similar driving conditions.

3. **Adaptation based on feedback from SOC**:
   This approach is built up on the idea of changing the value of the equivalence factor depending on the variation of SOC with respect to the target value. The computation is made without past information or driving pattern prediction. An example of adoption of this approach is reported in [14].

2.3 Advanced Driver Assistance System

Advanced Driver Assistance System (ADAS) is a set of technologies that have been introduced in vehicles to reduce the driver's duties, with the aim of obtaining a more efficient, safe and comfortable driving behaviour. Therefore, ADAS are used both in normal driving conditions and in emergency situations.
These systems obtain information from the external world through sensors.
The main sensors used by ADAS are: [15]

- **Cameras**: mostly used to detect lanes, vehicles, pedestrians and objects, but they cannot estimate the distance from the detected element.
- **Radars**: emit high frequency waves and measure the change of frequency in the wave reflected from the object. This measurement is used to estimate the object's distance.
- **Light Detection And Ranging (LIDAR)**: also this type of sensor is used to detect the distance from an object. Lidars emit a laser signal and use the reflected signal to estimate the distance of an object.
- **Ultrasound sensors**: mostly used for short distances, they can detect the presence of objects using ultrasound waves.

There are many ADAS applications that have been developed. Some of them are:

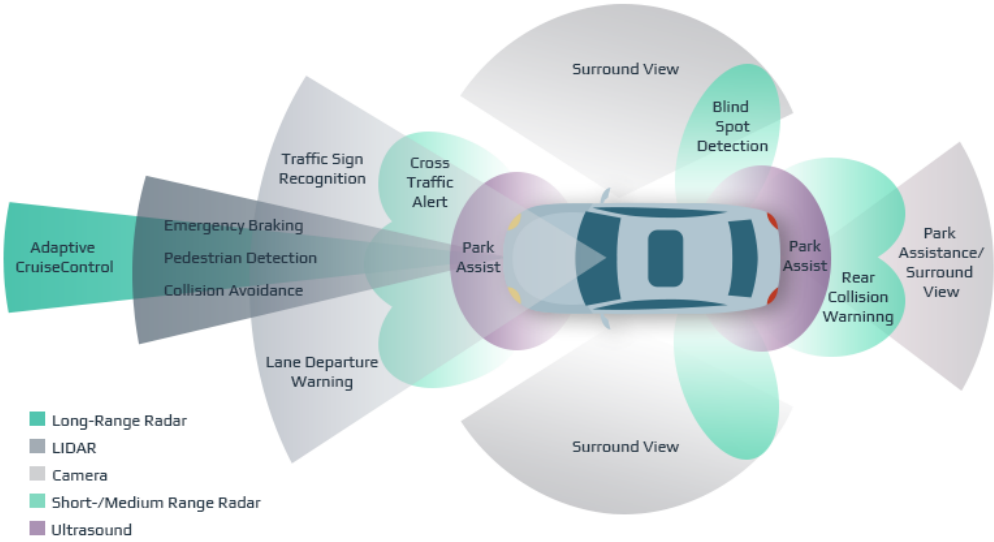

Figure 2.9: ADAS equipment on a vehicle

- **Adaptive Cruise Control (ACC)**: ACC is able to regulate the speed of the vehicle based on the velocity and distance of the preceding one.
  Therefore, it is useful to prevent accidents because it helps keeping a safe distance. In addition, this technology controls the acceleration and deceleration values, resulting in more efficient and comfortable driving behaviour.

- **Autonomous Emergency Braking (AEB)**: AEB can measure the distance from the objects ahead of the vehicle and it can act on the braking sensors to decelerate to avoid a potential crash.

- **Blind Spot Detection**: through the use of cameras and ultrasound sensors the system is able to detect the presence of objects in the so-called blind spots of the vehicle. The system can alert the driver.

- **Automatic Parking**: a development of Blind Spot Detection, it helps the driver in parking maneuver detecting objects and distances. In some vehicles the maneuver is completed autonomously

by the vehicle.

- **Lane Departure Warning**: this application uses cameras to detect whether the vehicle is within the marked lanes. In case of departure from the lane, the system alerts the driver.

2.3.1 ADAS regulation in Europe

In the Vehicle General Safety Regulation of November 2019 [16] the European Parliament introduced a range of mandatory ADAS to improve road safety for passengers, pedestrians and cyclists. These rules will apply on all the new vehicles from July 2024.
The mandatory ADAS established in this document are:

- For all road vehicles: intelligent speed assistance, alcohol interlock installation facilitation, driver drowsiness and attention warning, emergency stop signal, event data recorder and reversing detection.
- For cars and vans: additional technologies such as lane-keeping systems and automated braking.
- For buses and trucks: additional features for the prevention of collisions with pedestrians or cyclists and for recognizing blind spots, and tire pressure monitoring systems.

2.4 Verification and validation of ADAS

A major part of the development process for automotive safety-critical systems consists in the verification and validation. In the automotive business, the management of the production steps follows a V-shape diagram, as shown in figure 2.10. [17]

Verification is needed to confirm that the outputs of the system comply with the specifications. Therefore, if there is an error in the requirements, this cannot be noticed in this phase and the result is a faulty product. For this reason it is important to have a validation phase against the specifications, especially for certification purposes.

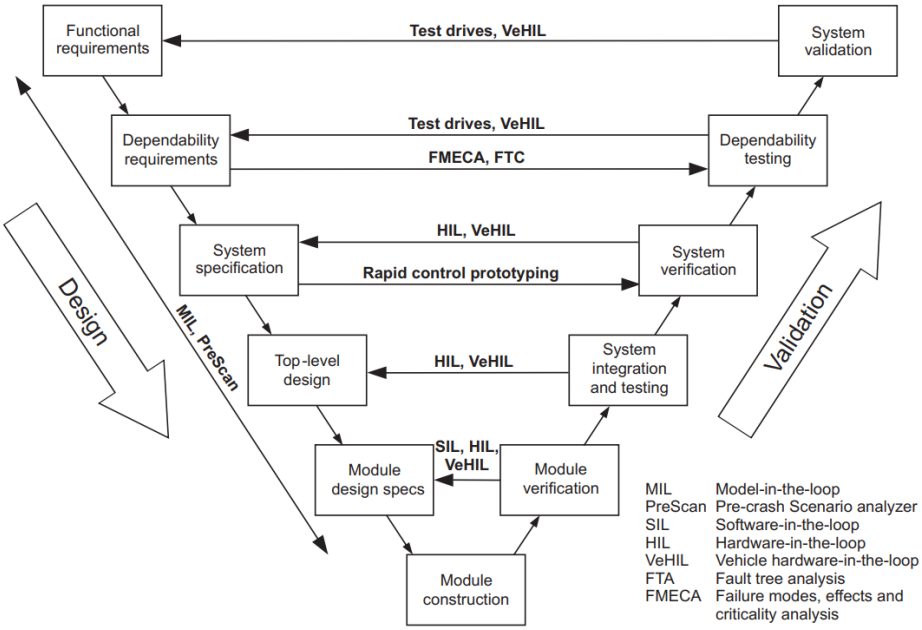

Figure 2.10: V-Shape diagram for the design and validation phases in the development of automotive safety-critical systems

Usually the verification and validation phases are iterated several times and the result of each iteration is used to modify the design of the system.
For this aim, *In-the-loop* simulation tools are always more appreciated for their fast and flexible results in the early-stage design of automotive control systems.

2.4.1 In-the-loop simulations

For the design and validation of ADAS control systems, different *In-the-loop* simulations are exploited.

The initial design of the system is performed with the support of *Model-in-the-loop* (MIL) simulations. For this purpose, there exist some off-line softwares that contain different modules that can be simulated in a run-time environment. An example of software that implements

these applications is Matlab.

- Control logic module: The ADAS control logic can be implemented taking also into account the sensors information. The parameters of the controller can be tuned to achieve the desired requirements. This can be done on the Matlab/Simulink environment.
- Vehicle dynamic module: The dynamics of the vehicle components (tyres, powertrain, sensors...) are implemented in the software. This can be done on Matlab/Simulink with the Simscape add-on.
- Environment module: The environment composed of buildings and roads, as well as actors such as cars and pedestrians, needs to be designed to test the system. On Matlab/Simulink the environment can be designed with the add-on Driving Scenario Designer.

When the results of the MIL tests are satisfying, the final product must be run in a real-time simulation to synchronize the tested components with hardware and software modules.
For the real-time test of the software, it is necessary to obtain the controller code using the automatic code generator of the MIL software. This code is then run in *Software-in-the-loop* (SIL) simulations, where it can be tested depending on the FPGA or processor used in the final hardware.
For the real-time test of the hardware, *Hardware-in-the-loop* (HIL) simulations are used. In this phase a combination of real and emulated components is tested. HIL simulations are well appreciated for their safe and flexible characteristic.
However, HIL tests have some flaws in the validation of the entire vehicle system due to the high cost and difficult repeatability of the conditions. In addition, the high system complexity reduces its controllability.[18]
To overcome these challenges, *Vehicle-Harware-in-the-loop* (VeHIL) simulations are introduced. In VeHIL a real vehicle prototype is tested in laboratory integrated with a HIL environment. The Vehicle Under Test (VUT) is placed on a chassis dynamometer that can emulate the road forces action on the actuators. Robot vehicles can be used to

simulate traffic scenarios.
VeHIL presents many advantages, especially for the lower cost since only one prototype vehicle is needed. In addition, since the environment is controlled through simulations, the repeatability of tests is assured. The benefit of this application is also the safety, because no humans is physically needed in the tests. [18]

Figure 2.11: Vehicle under test in VeHIL [17]

2.4.2 European New Car Assessment Programme

The European New Car Assessment Programme (NCAP) is an organization that rates the safety of new vehicles in Europe. It has many branches of testing and one of them is dedicated to ADAS. The system is tested on specific highway scenarios studied to prove the efficiency of the assistance technology in normal and critical situations.

2.5 Testing methodology: scenarios

In the development of ADAS it is important to verify the consistency of the system in the majority of possible traffic situations. To do this, it is useful to test the system on different scenarios as well as some driving cycles that represent typical speed profiles.
The testing of ADAS on critical scenarios is extremely important to understand the system behaviour especially in situations of potential accidents. The scenarios can be built taking into consideration different environment elements, that are subdivided into three categories by AIDE (Adaptive Integrated Driver-vehicle InterfacE) consortium [19]:

- Environment conditions: this category includes road type (urban, rural, highway...) and conditions (smooth, icy, bumpy...), as well as weather and visibility.
- Traffic conditions: this category includes the traffic situation and actors' presence, meaning vehicles but also pedestrians.
- Driving behaviour trajectories: this category includes the following of a trajectory related to specific driving actions, such as car following, overtaking etc.

For what concerns Adaptive Cruise Control, which will be the case of study of this work, the most relevant test scenarios are usually the ones that examine the system behaviour in the presence of other vehicles. These test cases can be used to verify that the ACC system satisfies safety and car-following requirements, such as for the NCAP Car-to-car tests [20], but also to show that fuel-economy and comfort are improved [21].
The most significant scenarios are reported in the following list.
The terminology used refers to "ego vehicle" (or Vehicle Under Test VUT) as the vehicle equipped with the system under test, while the "lead vehicle" (or Global Vehicle Target GVT) is the target preceding vehicle. The Time To Collision (TTC) is the time that the ego vehicle would take to strike the lead vehicle assuming that the two keep travelling maintaining the actual speed.

- **Car-following**: The system is tested on a ego car that follows a lead car with a specific trajectory. This scenario is not meant for the verification of critical situations but mostly for car-following and fuel-economy performance evaluation.

- **Cut-in**: In this scenario the ego car is travelling at a set speed or is following a GVT. A second vehicle changes lane and cuts-in moving into the same lane as the VUT, becoming the new GVT. The safety of the system can be tested in this case, verifying that the vehicle can decelerate and keep a safe distance from the new preceding vehicle.

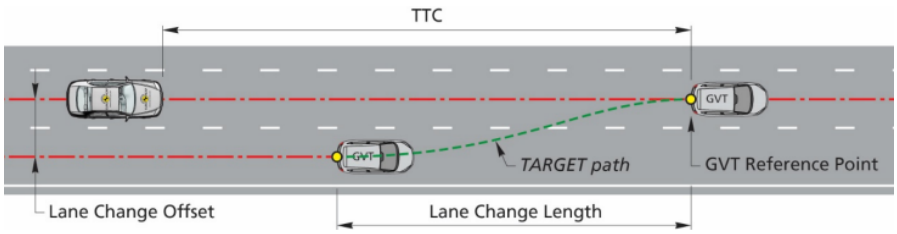

Figure 2.12: Cut-in scenario from NCAP tests [20]

- **Cut-out**: In this scenario the lead car changes lane. The ego car either finds a new lead car or travels at a set speed.

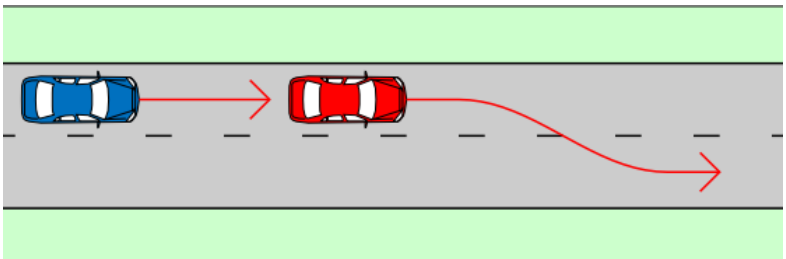

Figure 2.13: Cut-out scenario. In blue the ego vehicle and in red the lead vehicle [22]

- **Approach**: The lead car approaches a lead vehicle that is travelling at a lower speed or is stationary. The ability of the system to keep

a safe distance as well as the acceleration management for fuel-economy can be tested.

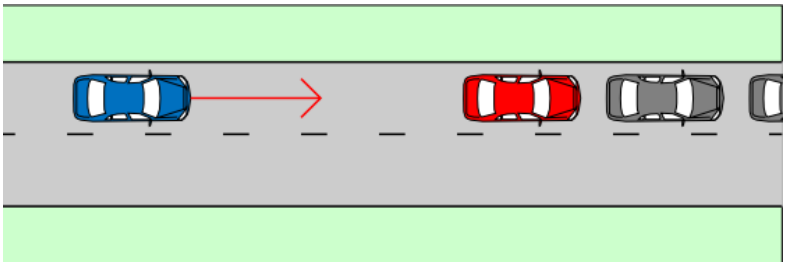

Figure 2.14: Approach of a stopped vehicle. In blue the ego vehicle and in red the lead vehicle [22]

- **Hard braking**: The lead car is following the ego car and this one suddenly brakes. The safety of the system is tested in this scenario, to ensure that safety distance can be kept also in situations of sudden speed decrement.

- **Fading**: The lead car is in car-following mode. The ego car starts to accelerate and overcomes the maximum target speed set for the VUT. Therefore the GVT fades away, getting out from the area that can be reached by the VUT sensors. The ego car keeps travelling at the set velocity without a preceding vehicle.

2.6 Case of study: Adaptive Cruise Control

ACC is a development of the more simple Cruise Control. As for this last controller, ACC can follow a velocity set by the driver, in the absence of other vehicles. In addition, when there is a preceding vehicle, it can adjust the acceleration based on its position and speed.
The data of the preceding vehicle is collected by sensors such as cameras or radars. If the system is composed of more than one type of sensor, the collected data can be combined through sensor fusion.

The longitudinal control system for ACC is generally based on a hierarchical architecture with two levels controllers. (Figure 2.15)
The upper level controller (decision-making controller) determines the

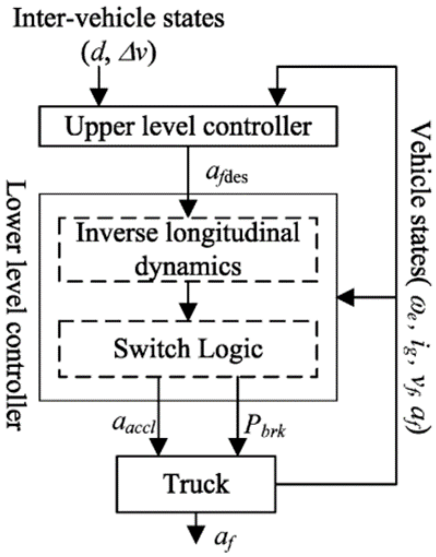

Figure 2.15: ACC hierarchical structure

desired acceleration so that the desired performances are met, based on the driver's settings and the driving information received by the sensors, such as distance and velocity of preceding vehicle. The lower level controller (underlying executive controller) determines the throttle and brake commands required to achieve the desired acceleration.
The choice of control strategy for the upper level controller is a deeply investigated topic in literature. Many researches focus on the best controller solution to minimize fuel consumption or to improve comfort.

2.6.1 ACC strategies to minimize fuel consumption (Eco-ACC): State of Art

Fuel consumption strongly depends on the values of acceleration. A driving behaviour with high values of accelerations and decelerations will lead to higher fuel consumption.

For this reason, ACC is exploited to regulate the value of acceleration taking into account efficiency objectives.
In literature there are many researches that study this application of ACC, called eco-ACC, using different types of control strategies. A few of them are explained below.

Model Predictive Control (MPC) is the approach preferred for fuel management. It can use speed control or space control and switch between the two modes based on real-time informations.
It can predict the future behaviour of preceding vehicles based on data collected through different ways. In [23] MPC is used combined with ECMS for a HEV. It estimates the battery energy profiles and uses it to anticipate the control of the electrical energy profile of the hybrid powertrain. The battery prediction profiles are calculated based on the road elevation and the vehicle speed controller. This research resulted in an improvement of fuel consumption of 9.6% compared to a vehicle with standard ECMS without ACC. However, this application can be used only in cases where the route is known a priori, otherwise it would not be possible to have information about the road elevation.
In [24] MPC is employed to follow an energy-optimal speed trajectory that is calculated offline by dynamic programming. Also in this case the route needs to be known a priori, so that the cloud can obtain the information about speed limits and road altitude to calculate the speed trajectory. In the online part the controller has to follow this trajectory while ensuring a safe distance from the preceding vehicle. (Figure 2.16). The demonstrated improvement expressed as energy consumption reduction with respect to a vehicle without ACC is 7.8%.

In [25] an MPC based ACC is exploited to achieve multiple objectives in vehicle-following mode. A quadratic cost function is developed to fulfill desired driver response, minimal fuel consumption and minimization of car following error. In addition, longitudinal ride comfort, driver permissible tracking range and rear-end safety are formulated as linear constraints. This method proved a fuel consumption improvement of 5.9% for urban scenarios and of 2.2% for highway scenarios, compared

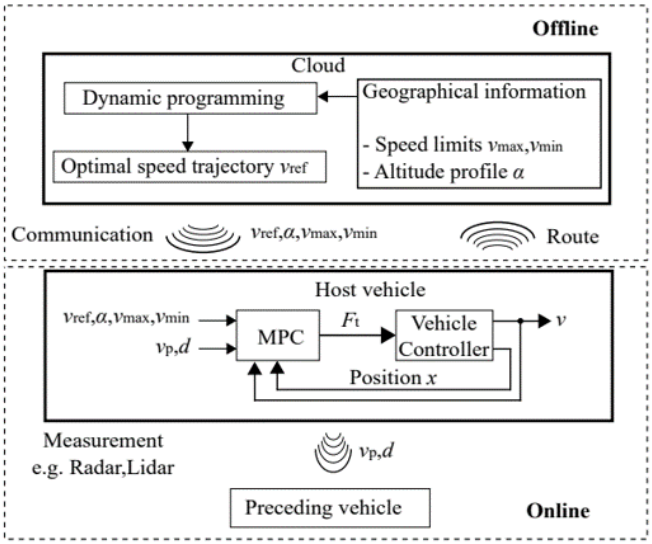

Figure 2.16: Scenario of the control strategy exploited in [24]

to a vehicle equipped with a standard ACC.

Fuzzy Logic (FL) is a strategy that seeks to imitate human drivers behaviour in car-following situations. However, this method must deal with too many parameters, and in [26] it is shown that in real-life driving situations it generally leads to non-optimal control. In [27] FL is compared to MPC and it is demonstrated that the first controller has a major fuel consumption. This is due to the fact that FL produces higher acceleration and deceleration values.

Adaptive Linear Quadratic Regulator (LQR) is another control strategy that has been investigated in literature. In [28] an algorithm for ACC based on Adaptive LQR was developed using a variable weighting on the acceleration, based on the relative distance and the acceleration of the lead vehicle. The main weakness of this method is that it does not put any constraint on collision avoidance. In addition, the study shows that when the algorithm is focused on vehicle-following performance the fuel consumption is high and vice versa.

In [29] a new application for fuel-economy is proposed, called "Sailing-ACC". This approach disengages the clutch when no torque is requested, exploiting the kinetic energy of the vehicle for travelling when propulsion is not necessary. The system switches between sailing and acceleration mode, generating a "pulse-and-glide" pattern. An optimization algorithm is developed to find the operating switch points that minimize fuel consumption. It was proved that this method leads to a saving of 43.4% of fuel in case of car-following scenario at around 40km/h.

Chapter 3

Model and strategy

3.1 Vehicle model overview

The starting model of this thesis work is a 48V P1 mild-hybrid IVECO Daily vehicle, implemented on MATLAB/Simulink/Simscape.
The modelization of a hybrid vehicle can be done following different approaches to predict power management. These methods can be classified based on the direction of the calculation, distinguishing between backward and forward.

- **Backward approach**: In this approach a driving cycle provides the target velocity, which is assumed to be followed perfectly. The vehicle's parameters evolve in time and the vehicle speed flows through the powertrain to the driver in an inverse way.

- **Forward approach**: In this approach the target speed passes through the driver and is given to the model as a torque request that tries to satisfy the desired velocity profile. This torque request propagates through the powertrain to the wheels in a forward way.

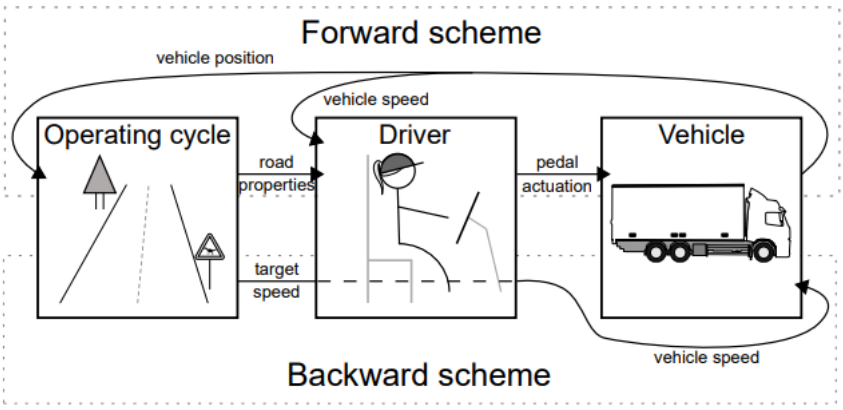

Figure 3.1: Forward scheme (on top) and backward scheme (on bottom) [30]

The model considered in this work is implemented following the forward approach, as shown in figure 3.2.

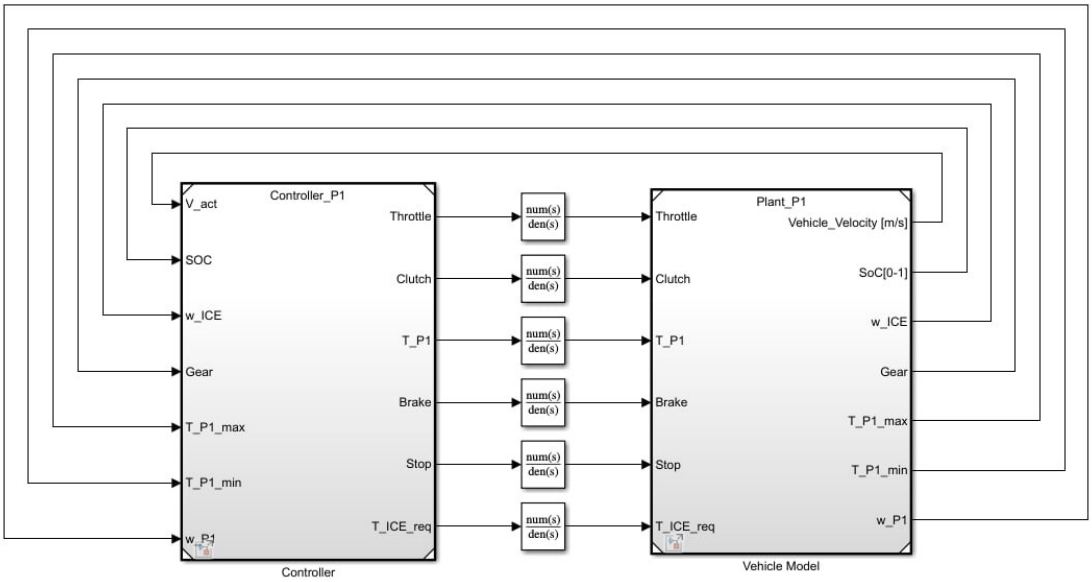

Figure 3.2: Forward model of the vehicle on Matlab/Simulink

3.1.1 Plant

The plant of the model, implemented on Matlab Simulink with Simscape add-on, is shown in figure 3.3. It contains blocks that represent the vehicle model and the tire model in a two-dimensional way, and the powertrain.
The longitudinal dynamics of the vehicle are schematized through a two-axle vehicle body accounting for body mass, road incline(which is considered null in this work), aerodynamic drag, and weight distribution between axles.

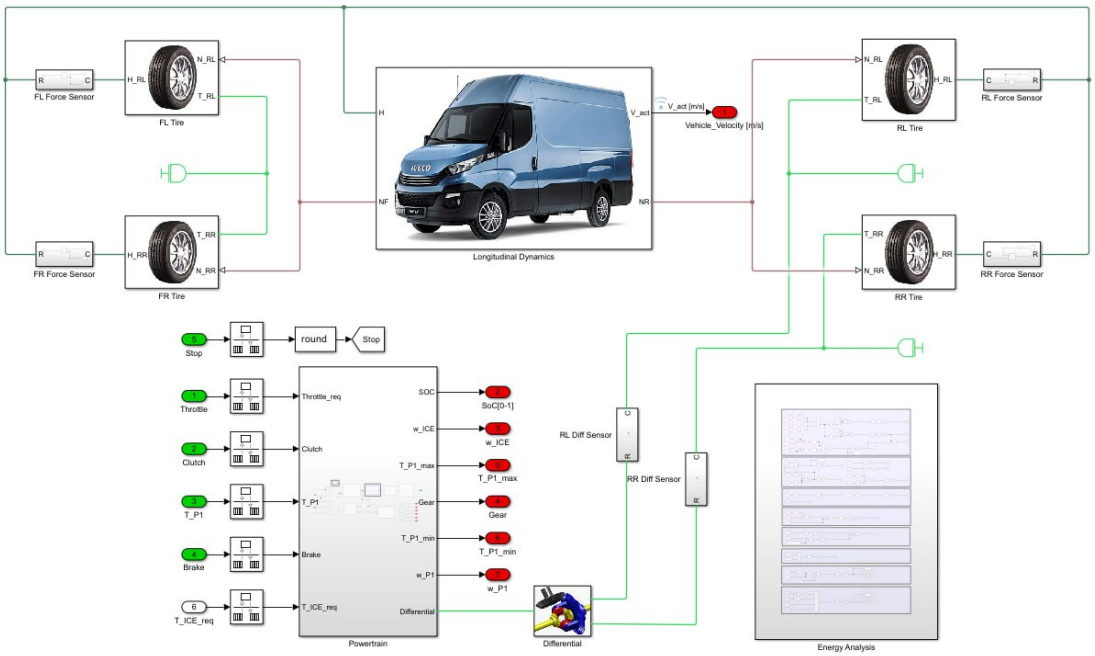

Figure 3.3: Plant of the model

Powertrain

In the powertrain model, shown in figure 3.4, it is possible to observe that the electric motor is positioned at the crankshaft of the ICE. Therefore, the powertrain layout is a P1 configuration.

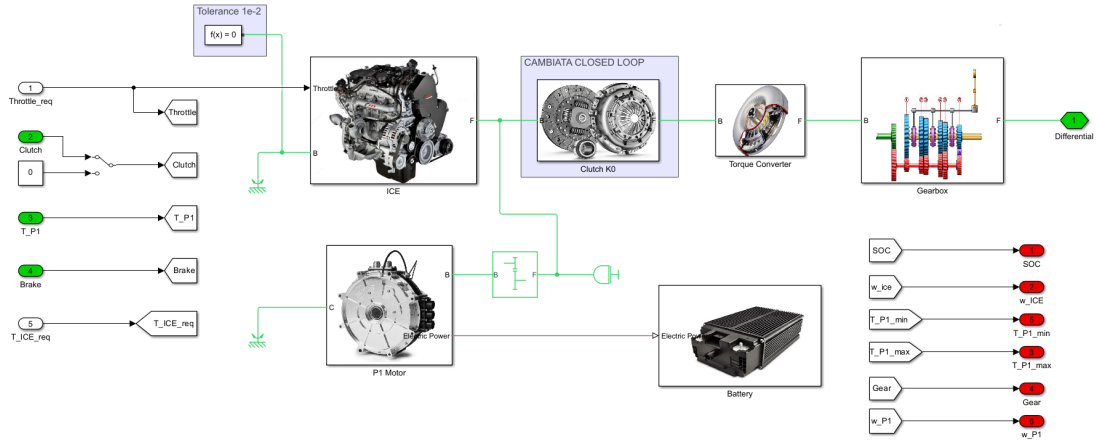

Figure 3.4: Powertrain model

3.1.2 Energy analysis of the powertrain

The focus of this thesis work is to improve the efficiency of the vehicle, decreasing the total fuel consumption. Therefore it is fundamental to analyze the powertrain energy flow to understand the actual losses and the total potential of energy recovery. Hence it is possible to know in which way the efficiency can be improved, and the best strategy can be found.

The considered vehicle is a mild-hybrid. This means that the primary source of energy is the ICE. The electric motor, connected to a small battery pack, is used to assist the engine in reducing fuel usage. These two motors have to satisfy the total energy requested for traction from the controller. For positive torque requests the EM operates in motoring mode, while for negative torque requests the EM operates as a generator and produces an electric energy that is stored in the battery. The total energy produced in the powertrain is given by the sum of the energy from the ICE and from the EM working in motor mode:

$$E_{powertrain} = E_{ICE} + E_{EM,motor}$$

This energy flows through the driveline to the differential. The driveline is composed of all the rotating elements and gears, and it transmits the power from the motors to the axle and thus to the wheels. However, the driveline's components dissipate some power due to internal losses, therefore the output energy is lower than the energy coming from the motors. These losses are represented by the following relationship, where $E_{differential}$ is the energy at the differential:

$$E_{powertrain} - E_{differential} = E_{driveline,losses}$$

The energy from the differential is transferred to the wheels and transformed into energy of motion, which is the energy needed by the wheels to move the vehicle. This energy should also compensate for the energy dissipated due to aerodynamic resistance, rolling resistance and potential energy, caused by the respective forces:

$$F_{aerodynamic} = \frac{1}{2}\rho_{air}A_f C_d v_{veh}^2$$
$$\mathrm{F}_{rolling} = c_{roll}(v_{veh}, p_{tire}, ...)Mv_{veh}gcos\delta$$
$$\mathrm{F}_{grade} = M_{veh}gsin\delta$$

Where $c_{roll} = c_{r0} + c_{r1}v_{veh}$ is a rolling resistance coefficient, ρ_{air} is the air density, A_f is the vehicle frontal area, C_d is the aerodynamic drag coefficient, g is the gravity acceleration, δ is the road slope angle. The values of these coefficients are reported in table 3.1

ρ_{air}	1.225
c_{roll}	0.0107
A_f	4.614
C_d	0.46
δ	0

Table 3.1: Values of dissipation forces coefficients in the model

The value of the losses strictly depends on the vehicle velocity, as it is possible to notice from the formulas. This behaviour can be observed

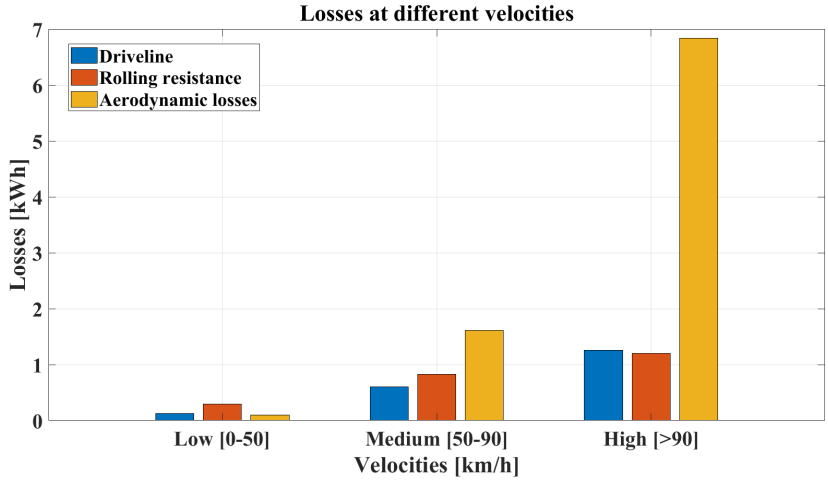

Figure 3.5: Energy losses related to speed

in the histogram (figure 3.5)where the energy dissipations related to the speeds of a complete driving cycle are reported.

The aerodynamic losses increase with high velocities, while at low speeds they are almost zero because the aerodynamic force is proportional to the square of the vehicle velocity. A similar behaviour is followed by the driveline losses that increase with the increase in speed. The losses due to rolling resistance are less relevant compared to the others.

Battery analysis

The battery is characterized by the following specifications 3.2:

Nominal voltage [V]	48
Cell capacity [Ah]	32
Nominal power [kWh]	1.5

Table 3.2: Battery specifications

The battery losses are computed as the difference between the output and the input power of the battery, where the input power is the electric power coming from the P1 motor:

$$P_{battery} = P_{P1,el} = P_{losses}$$

where $P_{battery} = VI$
The power of the P1 motor can be divided between electric and mechanical, defined as:

$$\begin{cases} \mathrm{P}_{P1,el} = P_{P1}\eta_{EM}^{sign(-P_{P1})} \\ \mathrm{P}_{P1,mech} = T_{P1}\omega_{P1,mech} \end{cases}$$

The difference between the mechanical and electric power of P1 are the losses of the electric motor:

$$P_{P1,mech} - P_{P1,el} = P_{loss,EM}$$

An important parameter for the battery analysis is the C-rate, which is a measure of the rate at which a battery is discharged, relative to its maximum capacity.
Knowing that the considered battery has a capacity of 32 Ah, it can discharge 32 A of current in 1 hour. Considering the nominal energy of 1.5 kWh, it can discharge 1.5 kW in 1 hour.
However, power electronics limitations must be taken into consideration. In this case, the components limit the current to around 400A, so a maximum C-rate of 15C can be considered.
The battery current of the considered vehicle has been analyzed on a complete driving cycle that takes into account urban, rural and highway driving situations. The profile, reported in figure 3.6, shows that there are some points where the current goes beyond the limits of 15C. These points correspond to sudden changes in the slope of the acceleration, that cause high torque requests.
Therefore, from this analysis it emerges that a better control of acceleration profiles would benefit the efficiency of this model also in terms of electrical energy management, as well as fuel usage reduction.

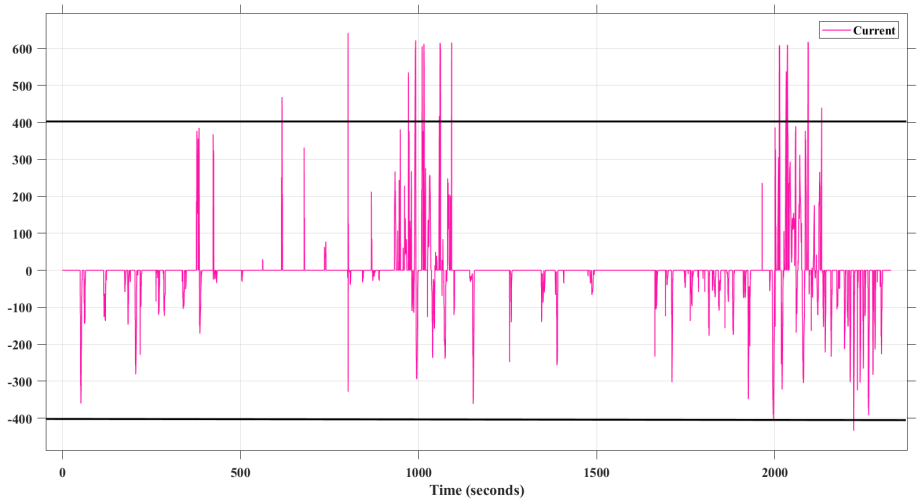

Figure 3.6: Battery current profile. The black lines indicate the current limit due to C-rate and power electronics restrictions.

3.1.3 Controller

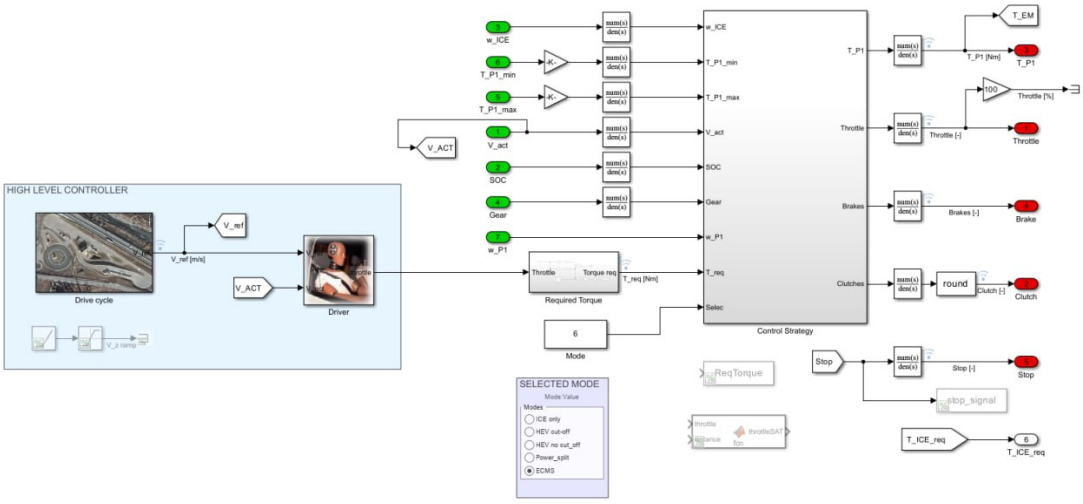

Figure 3.7: Controller model

The controller of the model, shown in figure 3.7, is composed of a high-level controller and a control strategy block for power management. In the high-level controller, the reference speed profile of a driving cycle is

given to the driver block.
The driver is modeled as a simple PI controller (figure 3.8) that needs to regulate the throttle to follow the speed profile. The equation that controls the output command is the one of a PID (Proportional, Integrative, Derivative) with the derivative term set to zero and the other parameters tuned to reach the desired output.

$$C = K_P + \frac{K_I}{s} + \frac{K_D s}{s+1}$$

Gain	Value
Derivative K_D	0
Proportional K_P	0.54
Integral K_I	0.03

Table 3.3: PID parameters

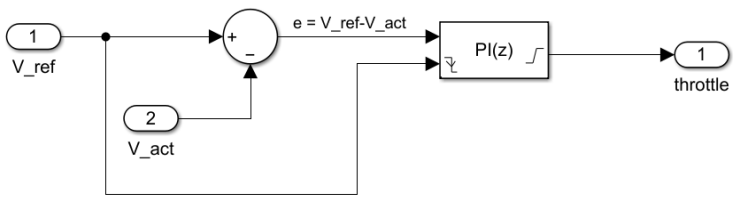

Figure 3.8: Driver PI controller

The output throttle command from the driver is then transformed into a torque request to be managed by the control strategy block to handle the power splitting method of the powertrain. For this scope, the model can work either in ICE only mode or in hybrid mode.
In the ICE only mode, the torque request is entirely fulfilled by the heat engine so there is no need for a power split strategy.
On the other hand, in the hybrid mode the torque request is fulfilled by both the ICE and the EM, therefore a management strategy for the power splitting is necessary. Among the several possible strategies, the

ECMS is the one chosen in this work.
This strategy handles the torque request by identifying two possible cases:

- If the torque request is negative, the EM works as a generator and produces an electric energy that is used to recharge the battery. This happens when the vehicle is braking.

$$T_{requested} \leq 0 \Rightarrow T_{requested} = T_{P1,generator}$$

- If the torque request is positive, the EM works as a motor and together with the ICE it contributes to supplying the total requested power.

$$T_{requested} > 0 \Rightarrow T_{requested} = T_{P1,motor} + T_{ICE}$$

This strategy also controls the management of the battery energy flow. Batteries can work in two different modes: Charge Depleting (CD) and Charge Sustaining (CS).
The Charge Depleting mode is mostly used in plug-in hybrid vehicles. At the beginning of the driving cycle, the battery is fully charged, while at the end the SoC is lower and the battery can be recharged from the grid.
In Charge Sustaining mode the battery SoC is maintained between an upper and a lower limit. The battery is discharged when the EM is working in motor mode, while it is recharged through regenerative braking while the EM is in generator mode.

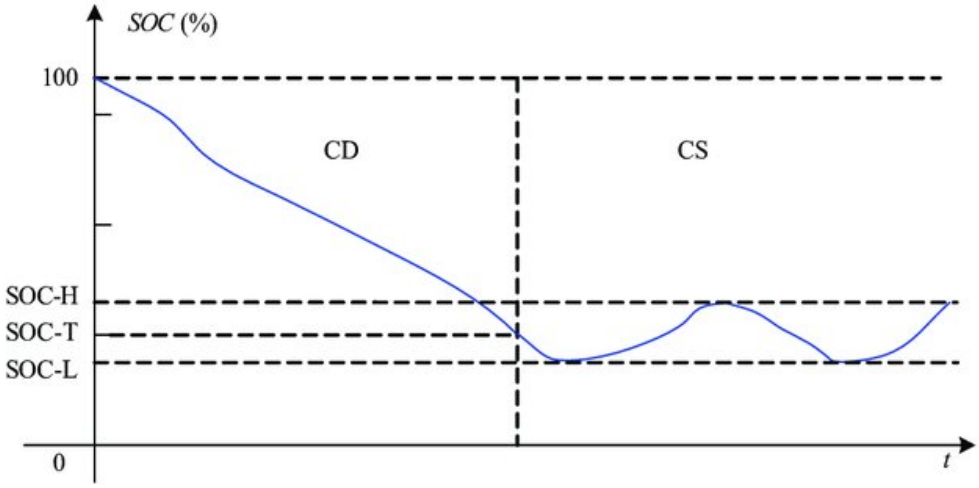

Figure 3.9: Charge Depleting and Charge Sustaining modes of a battery. [31]

In the model considered in this work the battery is in Charge Sustaining mode. The lower and upper limits for the SoC are set respectively at 56% and 64%, and the target level is 60%.
As mentioned in paragraph 2.2.1 the key point of ECMS is the choice of factor s. Here the equivalence factor has been designed keeping into account the limits for CS mode, defining a relay block that has as input the SoC and as output s.

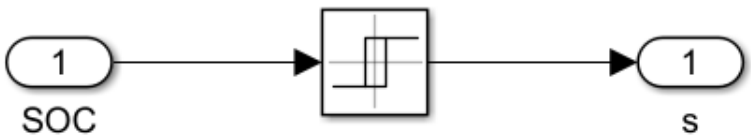

Figure 3.10: Relay block for equivalence factor evaluation

This relay turns on when the SoC overcomes the upper limit of 64%. After this, the relay remains on until the switch-off point is reached, meaning 56% SoC. The relay will stay off until the switch-on point is

reached again.
The equivalence factor evaluated in this way is given as input to the ECMS, which can manage the torque split also based on the SoC.
If the SoC is higher than 64% the torque is given only by the P1 motor so that the SoC can be brought between the desired limits. On the other hand, if the SoC is below 56% only the ICE contributes to the torque so that the battery can recharge.

3.1.4 Efficiency maps

Efficiency maps are used to understand the performances of the motor in different operating points in the torque-speed plane. They are employed for both internal combustion engine and electric motor.

ICE efficiency map

For the internal combustion engine, the efficiency map is represented in terms of brake specific fuel consumption (BSFC). The efficiency of the engine is evaluated by dividing the total fuel consumed $\dot{m}_f$, measured with a dynamometer as mass flow rate, by the engine input powerP_e:

$$BSFC = \frac{\dot{m}_f}{P_e} \tag{3.1}$$

Since the engine power is the product of engine speed w_e and torque T_e, equation 3.1 can be rewritten as:

$$BSFC = \frac{\dot{m}_f}{w_e T_e} \tag{3.2}$$

The BSFC can be represented as a contour plot in the speed-torque plane. Usually, the lowest BSFC can be found at mid-engine speeds and high torque.
In figure 3.11 it is reported the BSFC map of the ICE motor used for this work.

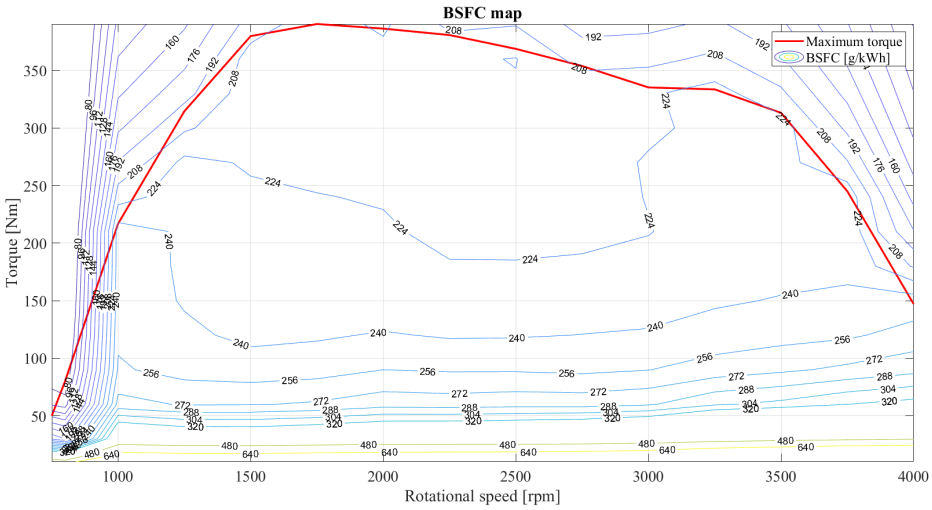

Figure 3.11: BSFC map

EM efficiency map

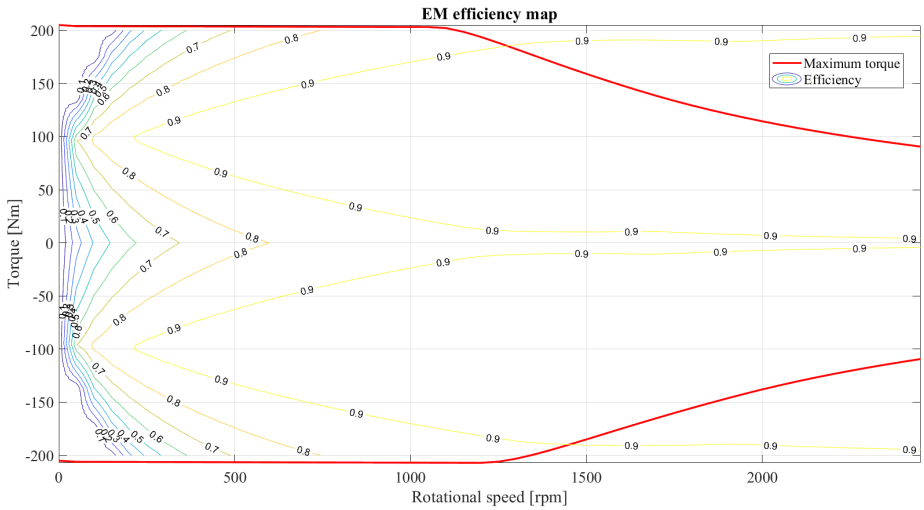

Figure 3.12: EM efficiency map

For the electric machine, the efficiency map is a plot of the maximum efficiency values in the speed-torque plane. The torque can either be positive (when the machine is working in motor mode) or negative

(when the machine is working in generator mode).
The efficiency map of the EM used in this work is represented in figure 3.12, where the represented data was obtained experimentally:

3.2 ACC controller

The focus of this thesis work is to exploit ADAS to reduce fuel consumptions. In particular, the chosen case of study is the ACC technology. This ADAS application can regulate the acceleration values resulting in a more efficient driving behaviour, as better explained in section 2.6. Therefore, the Driver block in the Simulink model needs to be substituted with an ACC block that, given the reference velocity of the preceding vehicle, calculates the optimal value of acceleration.

3.2.1 Starting model: Mathworks ACC with Sensor Fusion

The ACC designed in this work starts from a Mathworks example that models Adaptive Cruise Control with sensor fusion [32]. This example was then modified and integrated in the IVECO Daily model.

The starting model is composed by two main blocks, one with the design of ACC with sensor fusion and the other one that models the vehicle dynamics and environment. (Figure 3.13)
The first block integrates the data obtained with camera and radar sensors to detect the preceding vehicle, and calculates the relative distance and velocity. These values are then given to the ACC algorithm block to evaluate the desired acceleration for the ego vehicle. This algorithm was suitably modified, as it will be explained in the next section, to obtain an improvement in fuel-economy and car-following performances.

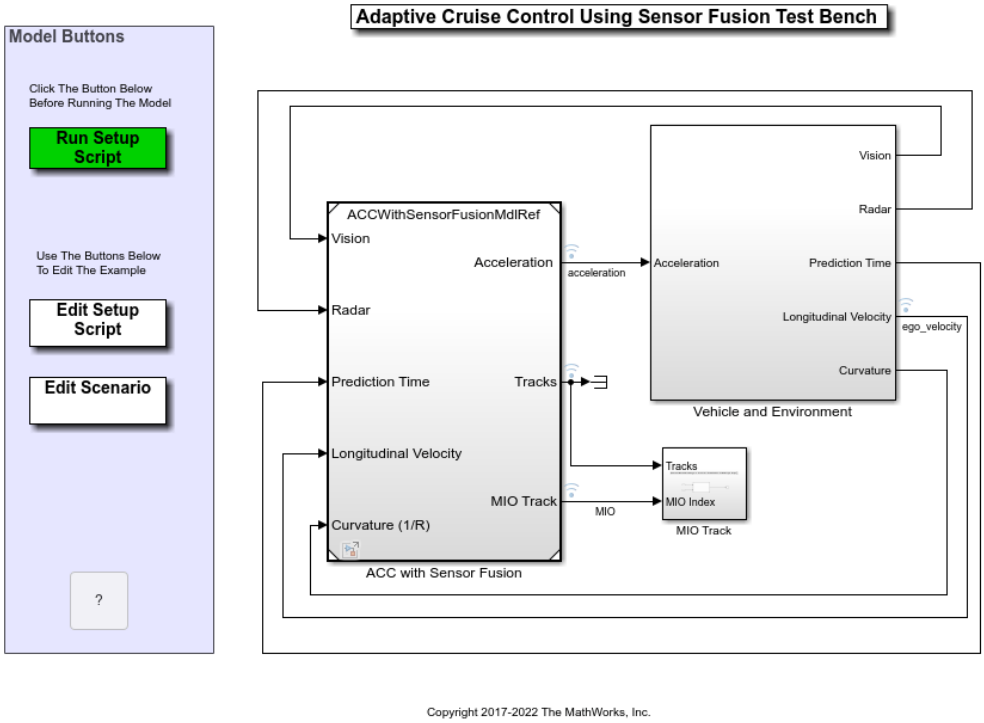

Figure 3.13: ACC with Sensor Fusion Mathworks model testbench

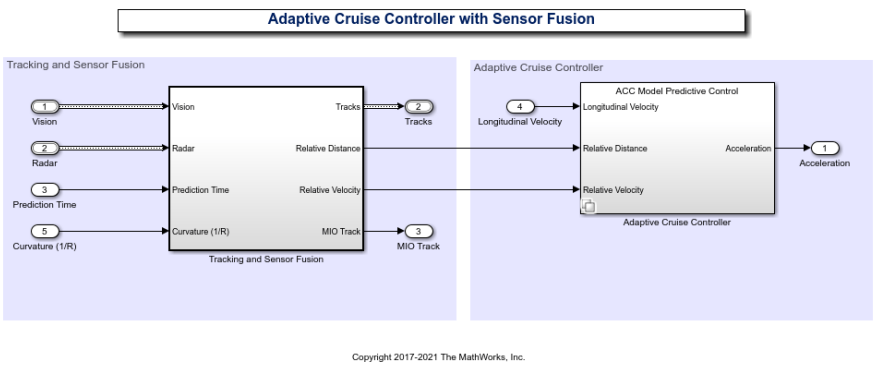

Figure 3.14: ACC with Sensor Fusion Mathworks model

The Vehicle and Environment block models the vehicle as a bicycle model, while for the environment it considers a curved road with different actors, with a scenario designed on the Matlab Driving Scenario Designer add-on.

3.2.2 Integration in the IVECO Daily model

To exploit the function of the ACC, the controller with sensor fusion has been integrated in the model substituting the driver in the high-level controller.

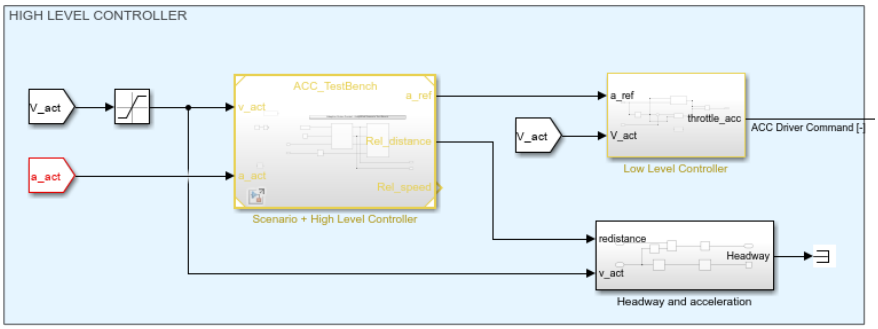

Figure 3.15: High-level controller with ACC

The new high-level controller is composed of two main different modules(Figure 3.15). The first one, which can be considered a high-level controller, is composed of the ACC model adapted and modified from the Mathworks example. The second one is a low-level controller that converts the reference acceleration command into a throttle command. The first block (Figure 3.16) is formed by a "scenario" reader block and by the actual Adaptive Cruise Control algorithm. The scenario module reads the data from the sensor and evaluates the distance and velocity of the preceding vehicle. The estimated values are used as input for the ACC system. This second block implements the actual high-level control algorithm. There are several algorithms that can be used for this application. This work focuses on the so-called Classical ACC strategy.

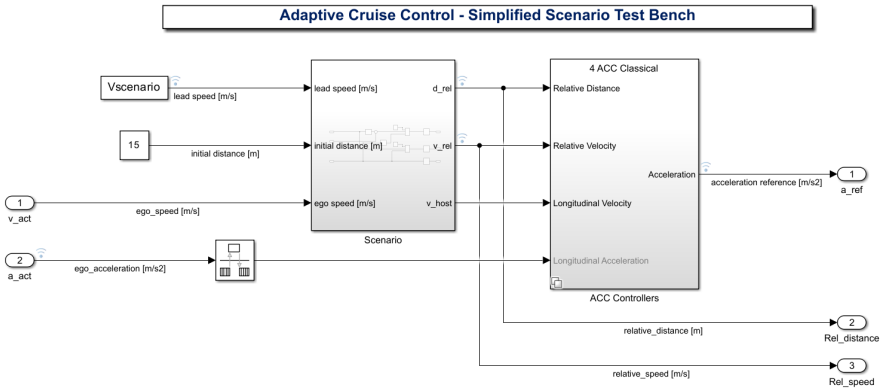

Figure 3.16: High-level controller with ACC and scenario reader.

3.2.3 Classical ACC

The Classical ACC develops an algorithm to maintain a constant time gap from the preceding vehicle during car-following mode. The ego vehicle travels at a driver-set velocity while maintaining a safety distance, defined as:

$$D_{safe} = D_{default} + V_{actual} T_{gap} \tag{3.3}$$

Where T_{gap} and $D_{default}$ are fixed values, defined in the Matlab script. The *time gap* T_{gap} represents the time that passes between the lead and ego vehicles as they go through the same point. It is measured between the front axle of the ego vehicle and the rear axle of the lead vehicle. If it is measured between the same axle it is called *headway time*.

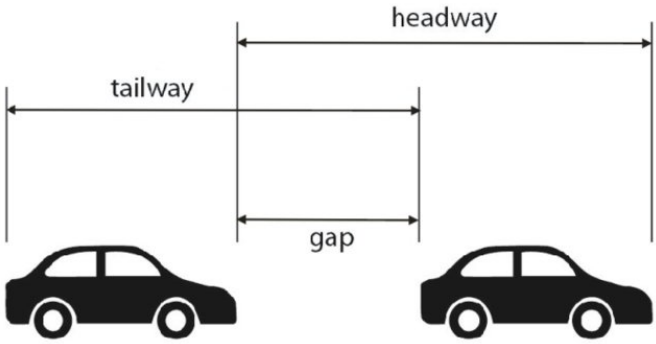

Figure 3.17: Time gap and headway graphic representation [33]

The default distance $D_{default}$ is the minimum desired distance that should be kept from the preceding vehicle.
V_{actual} is the actual longitudinal velocity of the ego vehicle.
The classical ACC implements a minimization problem to find the optimal value of acceleration to satisfy two main objectives: travel at a set velocity when the lead vehicle is far enough or slow down when the safety distance is not respected anymore.

$$min = \begin{cases} \mathrm{V}_{rel} v_{x,gain} - [D_{safe} - D_{rel}] x_{err,gain} \\ (\mathrm{V}_{set} - V_{act}) v_{err,gain} \end{cases}$$

V_{rel} and D_{rel} are respectively the value of relative velocity and distance of the preceding vehicle obtained from the sensor data.
The tuning parameters of this algorithm are the three gains:

- $v_{x,gain}$ is the gain on the relative velocity between the two vehicles.
- $x_{err,gain}$ defines the weight of the difference between the actual relative distance and the desired safety distance.
- $v_{err,gain}$ is the gain on the difference between the actual velocity and the set velocity

These gains can be tuned to give more or less importance to the relative parameter, based on the objective of the algorithm. The Classical ACC

can be tuned to satisfy car-following performance, or it can be less aggressive on that goal, leading to fuel-economy. In fact, the aim of this thesis work is not to follow perfectly the trajectory of the leading vehicle, but to use the information about its driving profile to optimize the driving efficiency of the ego vehicle. However, an equilibrium in the design of these parameters should be found to obtain acceptable performances on both sides.

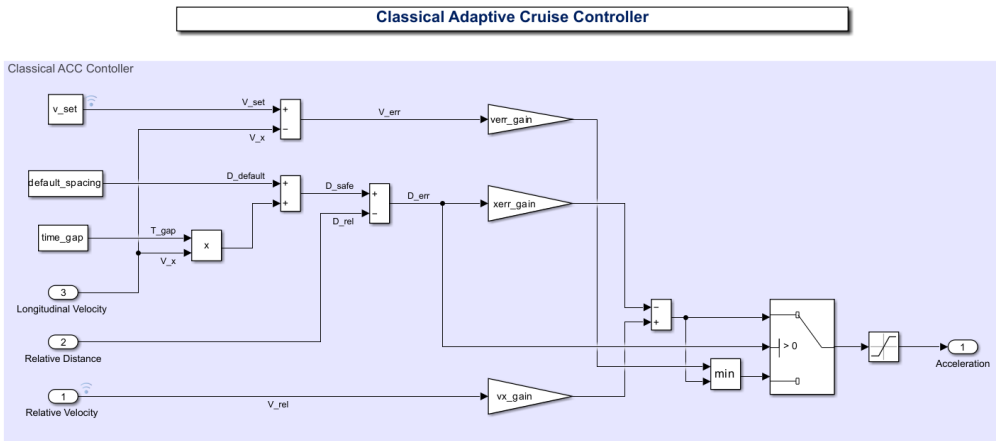

Figure 3.18: Classical ACC Simulink model

3.3 Tested scenarios

3.3.1 Driving cycles

Driving cycles are standard speed profiles that are used to test the behaviour of a system, especially for emissions verification. In this work they have been also exploited also to test the car-following behaviour, as they are a good representation of real-life driving situations, assuming that the leading car is following a standard driving cycle profile.
The United Nations Economic Commission for Europe (UNECE) has developed an approval procedure for light-duty vehicles with driving cycles based on statistical speed data on a flat road with no wind or other specific weather conditions. The tests are performed to obtain

information about fuel consumption and CO_2 emissions.
Three different cycles are used for these scopes: NEDC (New European Driving Cycle), WLTC (Worldwide harmonized Light vehicles Test Cycles), RDE(Real Driving Emissions).
Also in the United States, the Environmental Protection Agency (EPA) developed driving cycles for emissions evaluation. The Federal Test Procedure (FTP) and the US06 are two examples.

NEDC cycle

The New European Driving Cycle (NEDC) was introduced in 1992. It is composed by the repetition of an urban cycle (ECE-15 driving cycle) for four times, followed by a more aggressive Extra-Urban driving cycle. The first segment has a maximum speed of 50 km/h, while for the second one the maximum value is 120 km/h.

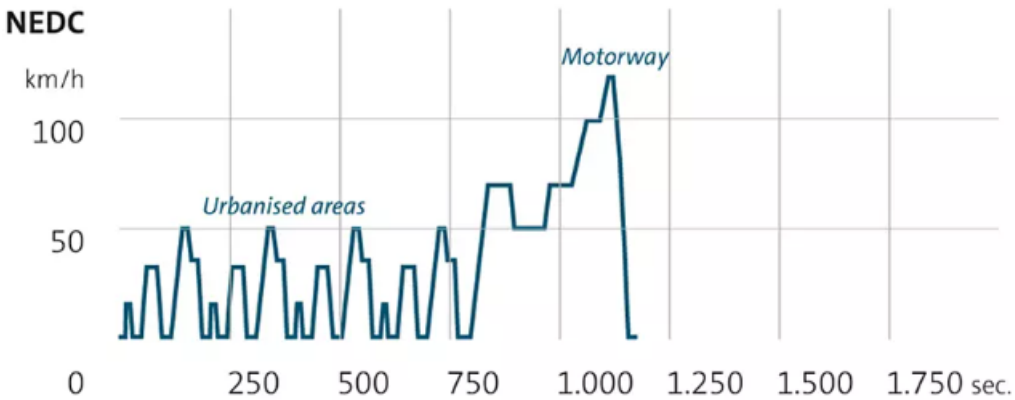

Figure 3.19: NEDC speed profile

The cycle parameters are reported in the following table [34]:

Distance [km]	10.9314
Total time [s]	1180
Average speed [km/h]	33.35
Maximum speed [km/h]	120
Average acceleration $[m/s^2]$	0.506
Maximum acceleration $[m/s^2]$	1.042

Table 3.4: NEDC parameters

WLTC cycle

The Worldwide harmonized Light vehicles Test Procedure(WLTP) is a set of procedures developed by the UNECE. It was introduced in 2017 to substitute the NEDC cycle, considered not realistic enough, especially in the acceleration values. WLTP includes different WLTC cycles mandatory in Europe for the emission tests of the categories of vehicles, sorted by power-to-mass (PMR) ratio. The considered categories are three:

- Class 1: low-power vehicles with PMR $\leq$ 22 W/Kg
- Class 2: vehicles with 22 W/Kg $<$ PMR $\leq$ 34 W/Kg
- Class 3: high-power vehicles with PMR $>$ 34 W/Kg

The cycle can be subdivided into four parts of increasing speed, for urban, suburban and highway scenario:

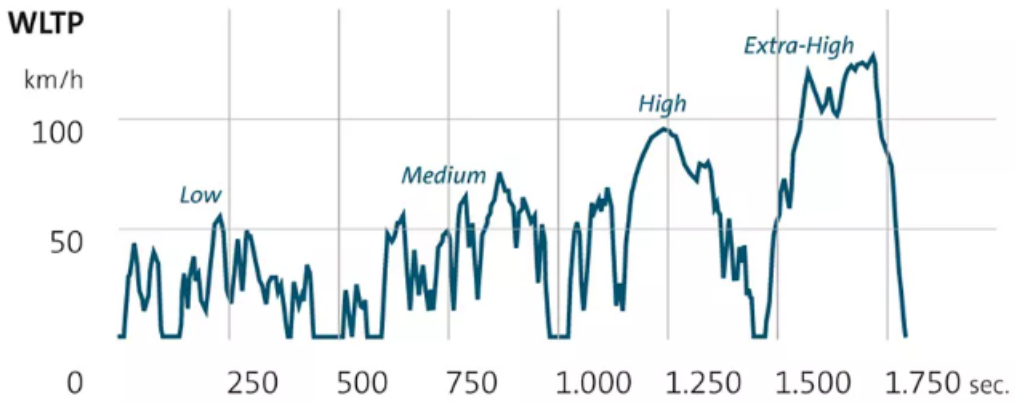

Figure 3.20: WLTP cycle

The cycle parameters are reported in the following table [34]:

Parameter	Low	Medium	High	Extra-high	Total
Distance [km]	3095	4756	7162	8254	23266
Total time [s]	589	433	455	323	1800
Average speed [km/h]	18.9	39.5	56.7	92.0	46.5
Maximum speed [km/h]	56.5	76.6	97.4	131.3	131.3
Maximum acceleration $[m/s^2]$	1.47	1.57	1.58	1.03	1.58

Table 3.5: WLTC parameters

It is possible to notice that the total distance is more than doubled with respect to the NEDC cycle. Moreover, the maximum speed is 131 km/h, against the 120 km/h of the NEDC cycle, which were not an exhaustive enough test. Also the average speed and maximum acceleration are increased in the new testing cycle.

RDE cycle

Real Driving Emission (RDE) cycle are introduced to test the vehicle emissions in real driving, and not only in test benches as in WLTC or NEDC. The cycle characterizes three different driving scenarios: urban, rural and highway. The urban one has a maximum speed of 60

km/h, the rural is between 60 km/h and 90 km/h and the highway is for velocities above 90 km/h up to 130 km/h. The specifications are reported in the table of figure 3.21 [35].

Trip specifics		Provision set in the legal text
Total trip duration		Between 90 and 120 min
Distance	Urban	>16 km
	Rural	>16 km
	Motorway	>16 km
Trip composition	Urban	29% to 44% of distance
	Rural	23% to 43% of distance
	Motorway	23% to 43% of distance
Average speeds	Urban	15 to 40 km/h
	Rural	Between 60 and 90 km/h
	Motorway	> 90 km/h (>100 km/h for at least 5 min)

Figure 3.21: RDE specifications

FTP-75 cycle

The Federal Test Procedure driving cycle was first introduced in the United States in 1978 to evaluate the emissions of light-duty vehicles. The FTP-75 driving test is a variation of the EPA Urban Dynamometer Driving Schedule (UDDS), which is a cycle that represents urban conditions. In the FTP-75 a phase of 505 seconds of urban cycle is added to the UDDS. The entire cycle is composed of 4 phases:

1. Cold start transient phase

2. Stabilized phase

3. Hot soak

4. Hot start transient phase

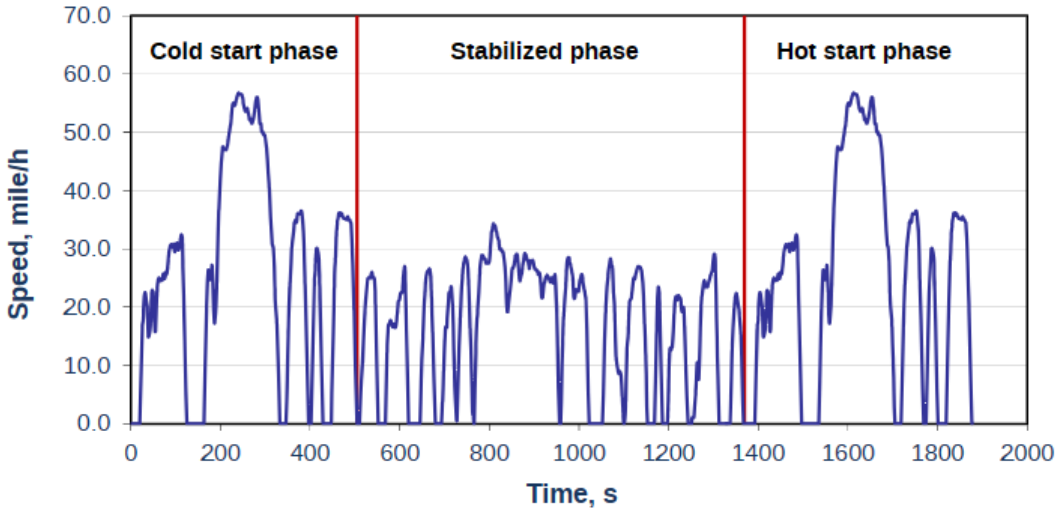

Figure 3.22: FTP-75 cycle [36]

The parameters of this driving cycle are reported in the following table :

Distance [km]	17.77
Total time [s]	1877
Average speed [km/h]	34.12
Maximum speed [km/h]	91.25
Maximum acceleration $[m/s^2]$	0.64

Table 3.6: FTP-75 parameters

US06 cycle

The US06 driving cycle was introduced as an integration of the FTP75 cycle, to represent a more aggressive driving behaviour, with higher accelerations and speed. The objective of this driving cycle is to evaluate performances and emissions also in non-urban scenarios.

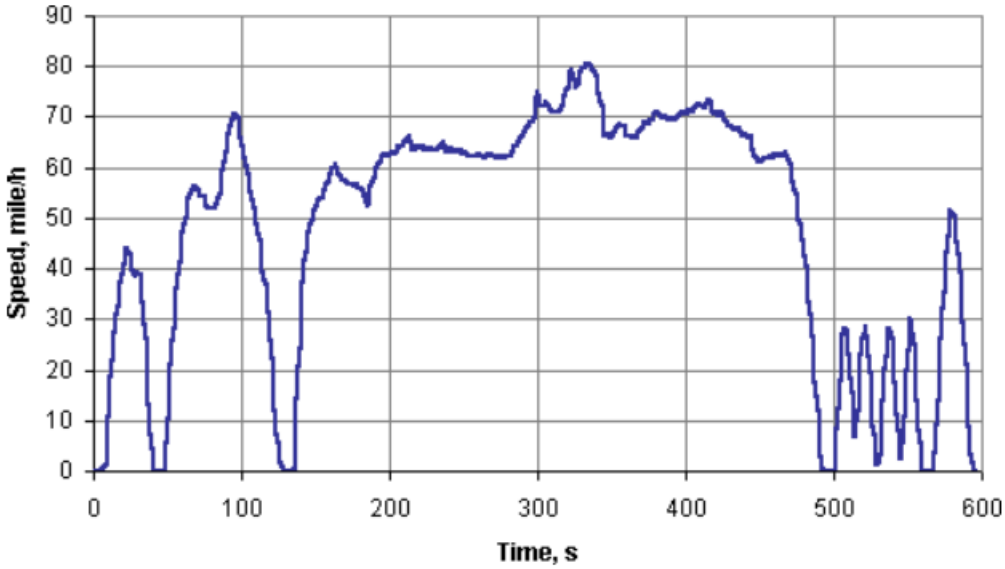

Figure 3.23: US06 cycle [37]

From the parameters of this driving cycle, reported in table 3.7, it is possible to notice that the maximum acceleration value is increased to 1.69 m/s^2, against the 0.64 m/s^2 of the FTP75.

Distance [km]	12.8
Total time [s]	596
Average speed [km/h]	77.9
Maximum speed [km/h]	129.2
Maximum acceleration [m/s^2]	1.69

Table 3.7: US06 parameters

Chapter 4

Simulations and results

4.1 Simulations strategy

To test the system, different driving cycles were used, reported in section 3.3.1. To study the behaviour of the system at different speeds, the RDE cycle was analyzed separating urban, rural and motorway segments. It was supposed that the ego car was following a lead car that travels according to the speed profile of the driving cycle. To evaluate the benefit of ACC, the results needed to be compared with the ones of the lead vehicle. To do so, the same speed profile was used as a reference for the ego car model not equipped with ACC, and the performances were compared.

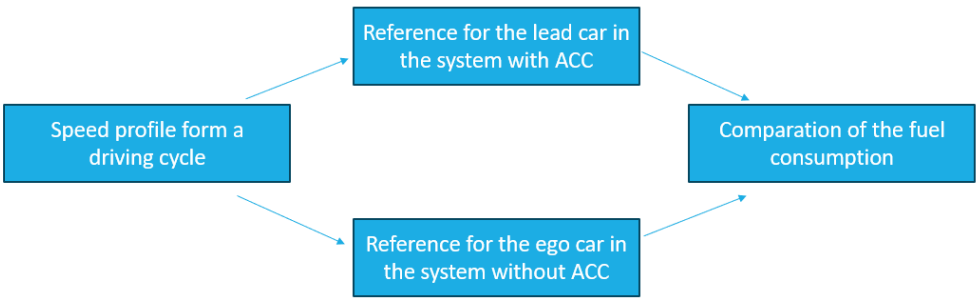

Figure 4.1: Simulation strategy

The ACC parameters were tuned to obtain good performances in terms of car-following behaviour, command stability and fuel consumption.
In particular, from the choice of the time gap derives the relative distance, so this parameter was tuned to respect the safety distance but also to stay within an acceptable maximum distance. In fact, if the lead vehicle is too far, it is outside the range of the ego car sensors and therefore it cannot be used as reference.
For all the simulations, the minimum safety distance was fixed, while the maximum acceptable value was established based on the speed:

Scenario	d_{min} [m]	d_{max} [m]
Urban	10	50
Rural	10	150
Motorway	10	250

Table 4.1: Safety distance thresholds

The testing strategy for all the simulations with ACC follows this flow:

1. *Verification of car-following parameters*: the ego and lead car should cover the same distance at the same time, so it is necessary to verify that:
   Δx_{lead}=Δx_{ego}
   Δt_{lead}=Δt_{ego}
   This means that the average speed of the two cars should be in the same range. The velocity of the ego car should be in the range of $\pm 10\%$ of the lead car speed profile.

2. *Evaluation of performances*: the performances of the system is evaluated in term of acceleration profiles and fuel consumption. In addition, the BSFC map of the ICE and the efficiency map of the EM are evaluated, to analyze the working points of the motor.

In section 4.3 the Classical ACC was integrated with a function that adapts the time gap based on the velocity.

4.2 Simulations on the system equipped with Classical ACC

The parameters of the ACC algorithm can be divided in two categories: fixed and tuning parameters. The fixed ones were chosen a priori, as reported in the following table:

Parameter	Value
$D_{safe}[m]$	10
$v_{set}[m/s]$	50

Table 4.2: Fixed parameters

The set velocity was established in order to ignore that parameter, so that the ego car can follow the lead car even at high speeds.
The gains were tuned after carrying out many tests to find the most suitable values to obtain a stable acceleration reference command.

Gain	Value
$v_{err,g}$	0.02
$v_{x,g}$	0.5
$x_{err,g}$	0.2

Table 4.3: Gains values

The gain $v_{err,g}$ was kept low to give a non-relevant weight to the set speed.
The value of time gap was tuned for each cycle to ensure the conditions explained in the previous section. This parameter should be low (around 2 seconds) to maintain good car-following behaviour. However, the results show that it is necessary to increase it for high speeds so that safety distance can be respected.

WLTC

For the WLTC cycle, the simulations were performed with time gap equal to 1.5 and 3 seconds, which were found as the best fitting choice, and the results were then compared.
The resulting speed profiles are reported in figures 4.2 and 4.3:

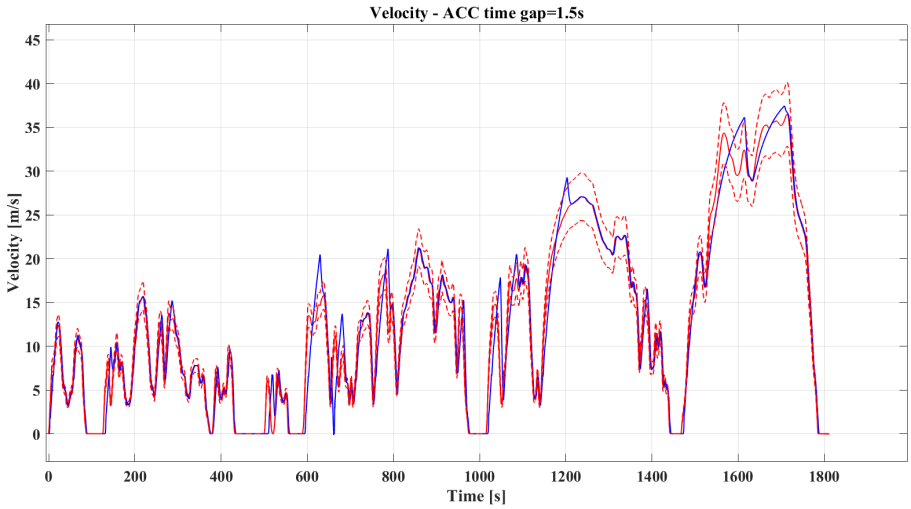

Figure 4.2: Speed profile for WLTC cycle, time gap = 1.5 s

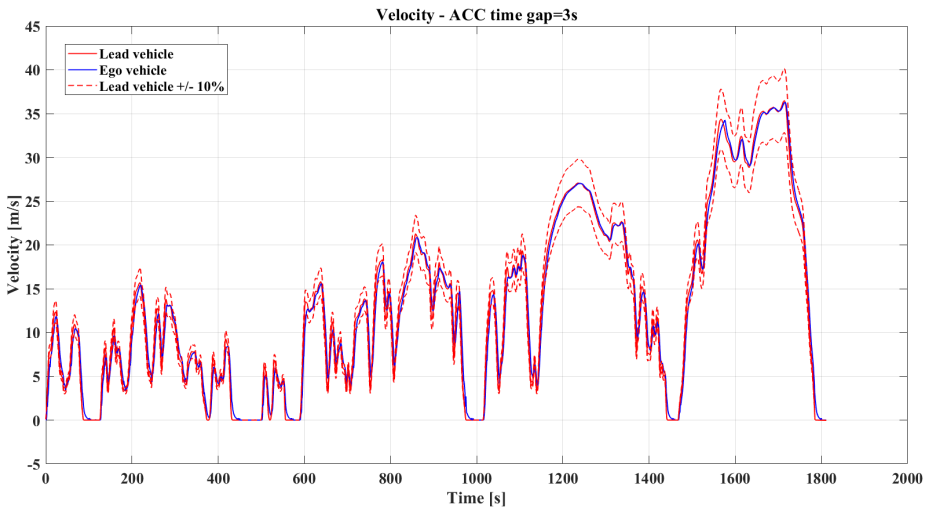

Figure 4.3: Speed profile for WLTC cycle, time gap = 3 s

The total covered distance and the deviation of speed from the lead vehicle profile are reported in table 4.4.
From these data it is possible to observe that for time gap equal to 3 seconds the car-following behaviour is in line with the expectations, while for time gap equal to 1.5 seconds there are some deviations from the lead car velocity. In fact, the acceleration profiles reported in figures 4.4 and 4.5 show that a lower time gap leads to a more aggressive controller, and this can result in some instabilities. The profile of accelerations is shown compared to the velocity, to better understand the controller behaviour.

Parameter	Time gap = 1.5 s	Time gap = 3 s	Lead vehicle
Covered distance [km]	23.27	23.27	23.27
Maximum deviation [m/s]	11.42	5.97	-
Average deviation [m/s]	1.02	0.62	-

Table 4.4: Car-following parameters in WLTC cycle

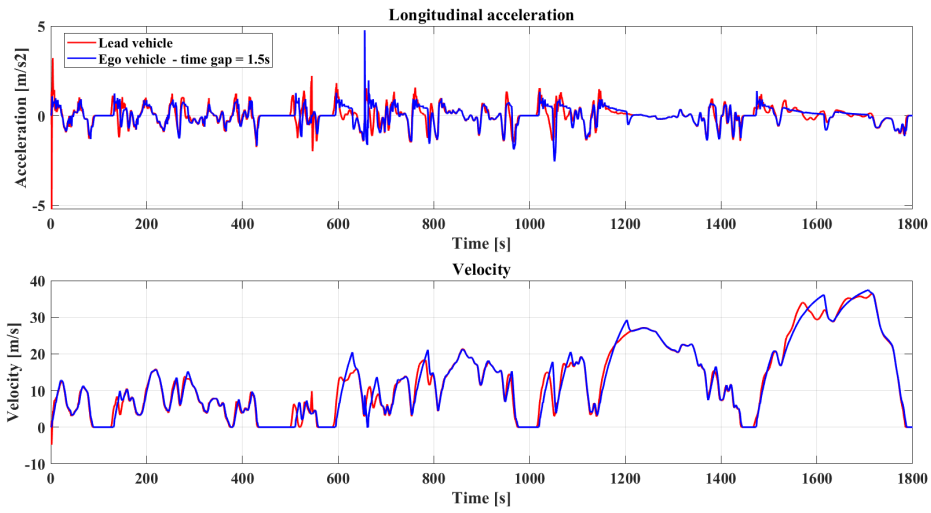

Figure 4.4: Acceleration and speed profile in WLTC cycle, time gap = 1.5 s

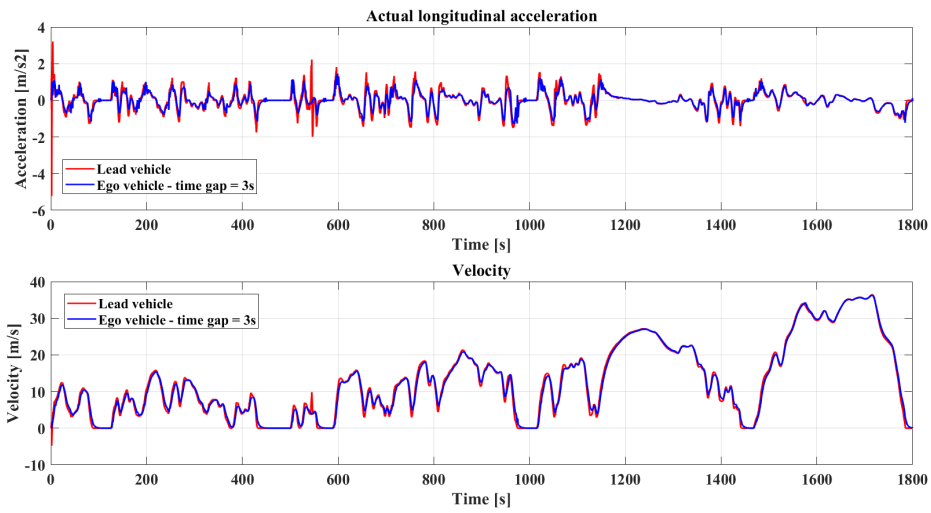

Figure 4.5: Acceleration and speed profile in WLTC cycle, time gap = 3 s

The relative distance is shown in figure 4.6.

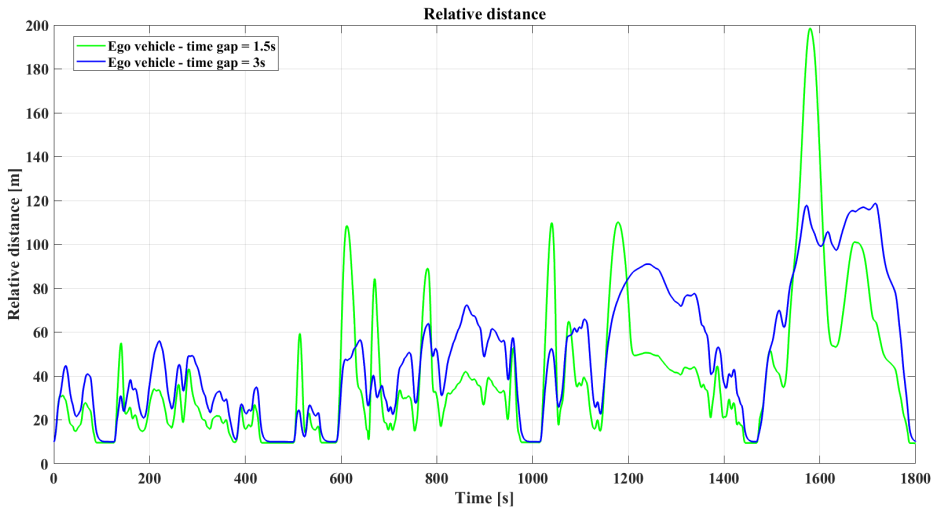

Figure 4.6: Relative distances in WLTC cycle

It is clear from these figures that the controller with time-gap equal to 3 seconds is more stable and leads to better car following performances. After verifying the satisfaction of these criteria, the efficiency of the

two controllers is evaluated, comparing it with the lead vehicle.

	Time gap = 1.5 s	Time gap = 3 s	Lead vehicle
Fuel consumption [l]	2.56	2.35	2.58
Improvement [%]	0.8	9	-

Table 4.5: Fuel consumption in WLTC cycle

The controller with time gap 3 seconds shows better behaviour also for what concerns the consumption, with an improvement of 9% with respect to the lead vehicle.
The BSFC map of the ICE (figure 4.7) shows that the working points of the controller with 3 seconds time gap are focused in an area with lower torque, and this also explains the lower fuel consumption.

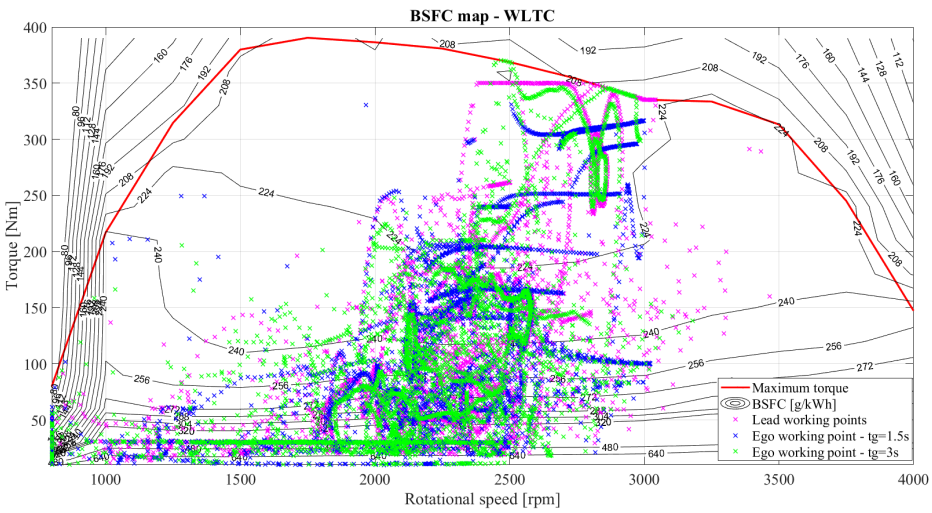

Figure 4.7: BSFC map in WLTC cycle

FTP75

The FTP75 cycle is a scenario that mixes urban and suburban speed profiles. However, from the tests it was proven that the minimum time gap that could respect the car-following requirements is 3 seconds,

especially for the safety distance upkeep. Therefore, the analysis of the system were all carried out considering 3 seconds time gap.
The velocity profile is within the desired range, and the relative distance is between the requested thresholds. The car-following parameters are satisfied.

Parameter	Time gap = 3 s	Lead vehicle
Covered distance [km]	17.77	17.91
Maximum deviation [m/s]	5.94	-
Average deviation [m/s]	1.04	-

Table 4.6: Car-following parameters in FTP75 cycle

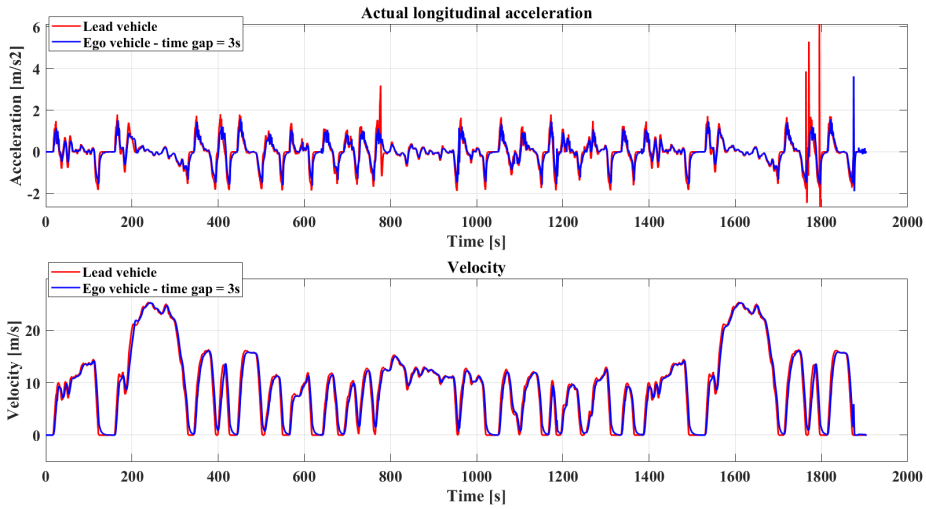

Figure 4.8: Acceleration and speed profile in FTP75 cycle, time gap = 3 s

Also the acceleration command has a stable profile, good for the efficiency of the system, which shows an improvement in the fuel consumption reported in table 4.7.

	Time gap = 4 s	Lead vehicle
Fuel consumption [l]	1.63	1.72
Improvement [%]	5.2	-

Table 4.7: Fuel consumption in FTP75 cycle

The efficiency map of the motor shows that the ego vehicle's working points are concentrated in a more restricted area, with lower torque requests and fuel consumption.

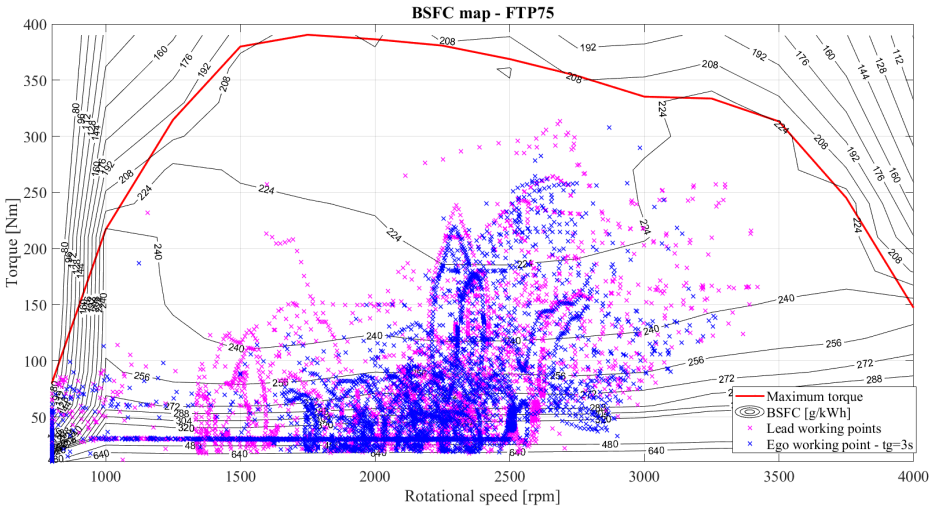

Figure 4.9: BSFC map in FTP75 cycle

RDE urban

The RDE urban cycle, like the WLTC and the FTP75, is characterized by smooth speed profiles that do not require high accelerations and decelerations, therefore also in this case a low time gap can be used. Also in this case the tests were performed with 1.5 and 3 seconds time gaps.
The resulting speed profiles are reported in figures 4.10 and 4.11.

The total covered distance and the deviation of speed from the lead vehicle profile are reported in table 4.8. The speed profiles are within

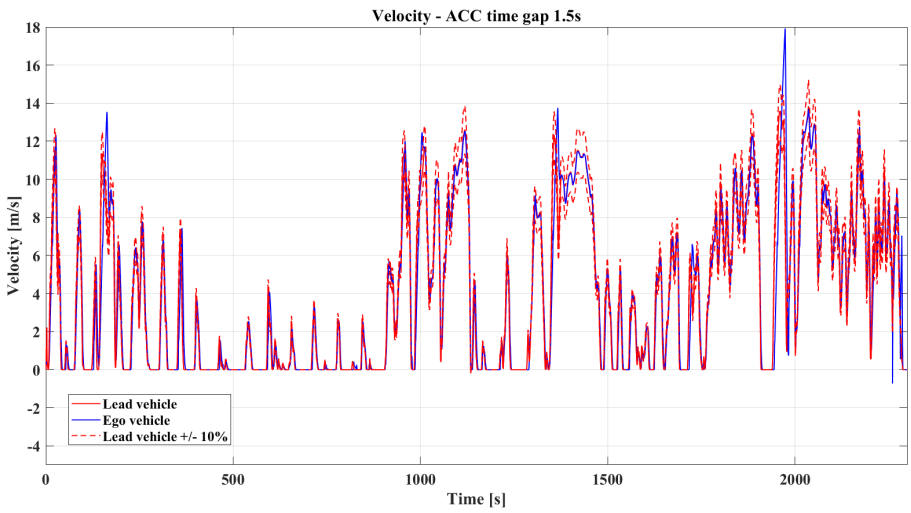

Figure 4.10: Speed profile for RDE urban cycle, time gap = 1.5 s

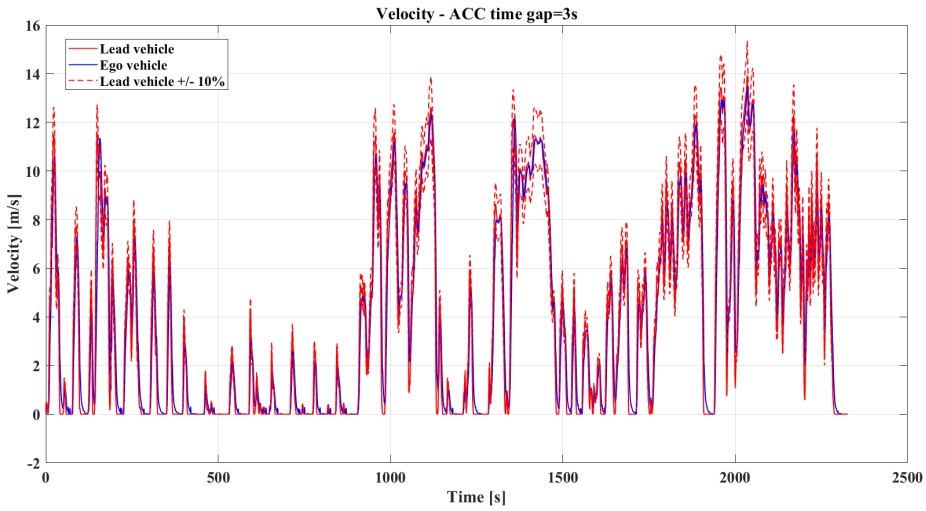

Figure 4.11: Speed profile for RDE urban cycle, time gap = 3 s

the 10% range of the lead velocity, and the covered distance is almost the same, so the hypothesis on car following performances are satisfied.

Parameter	Time gap = 1.5 s	Time gap = 3 s	Lead vehicle
Covered distance [km]	8.94	8.91	8.91
Maximum deviation [m/s]	10.44	6.32	-
Average deviation [m/s]	0.55	0.69	-

Table 4.8: Car-following parameters in RDE urban cycle

The relative distance between ego and lead vehicle is reported in figure 4.12, and it is within the maximum desired value established at the beginning of this chapter:

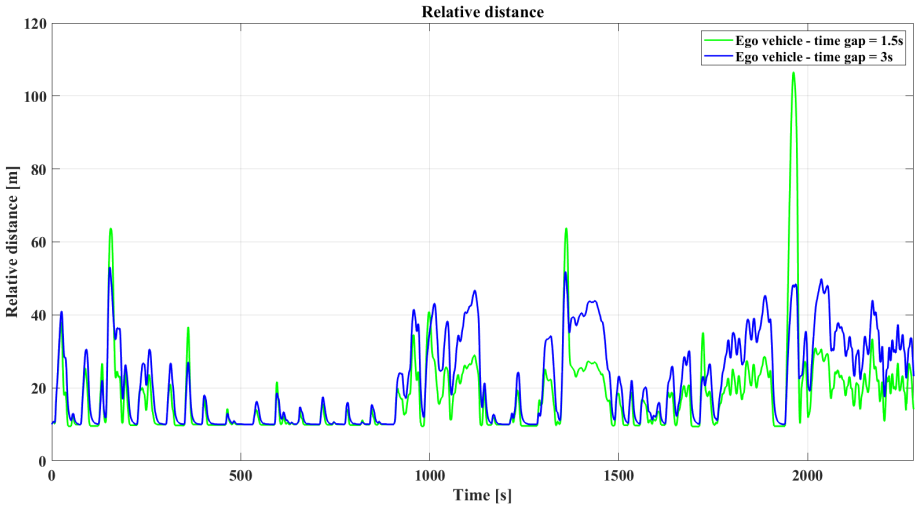

Figure 4.12: Relative distance for RDE urban cycle

Also in this case the controller with time gap equal to 3 seconds shows a better car-following behaviour.
Analyzing the acceleration profiles in figures 4.13 and 4.14 it is possible to evince that the ACC controller results in a smoother acceleration command with respect to the lead car not equipped with this technology.

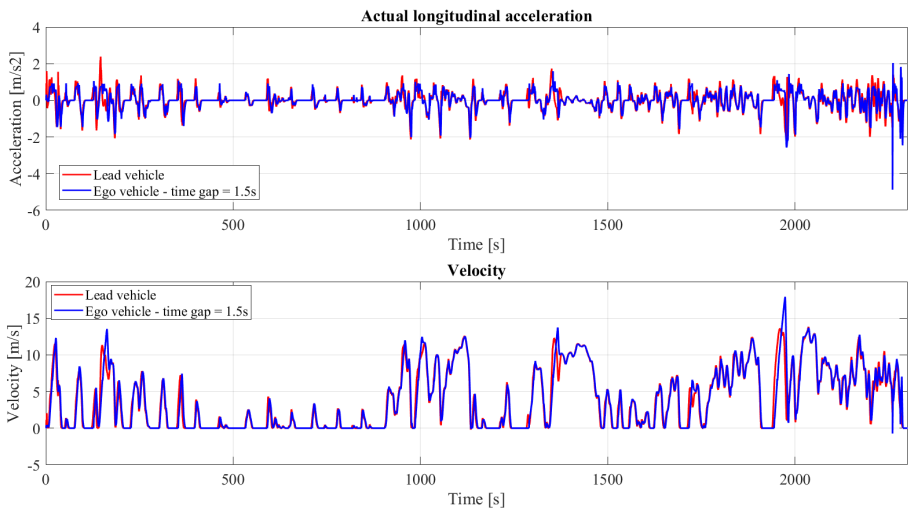

Figure 4.13: Acceleration and speed profile for RDE urban cycle, time gap = 1.5 s

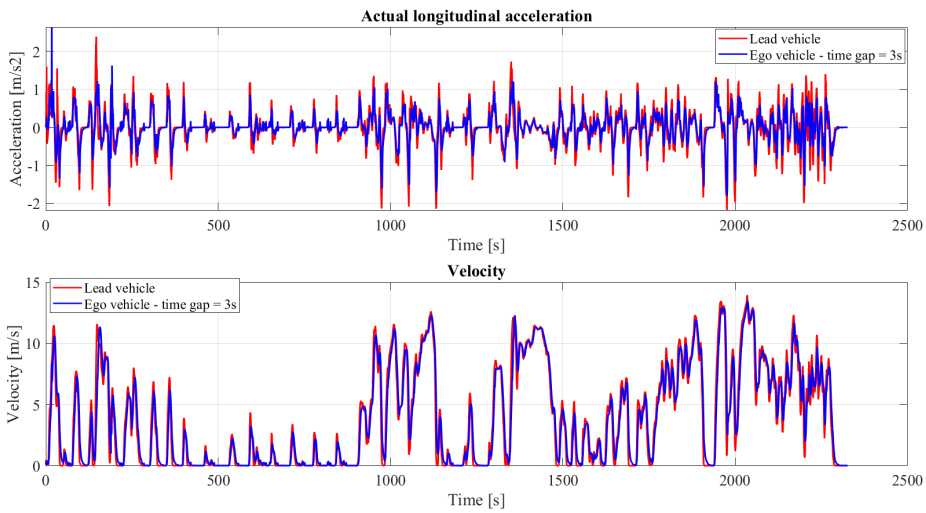

Figure 4.14: Acceleration and speed profile for RDE urban cycle, time gap = 3 s

The fuel consumption improvement, reported in table 4.9, shows a major enhancement using the controller with time gap equal to 3 seconds. A lower time gap does not show improvements because it is

more aggressive in car-following behaviour.

	Time gap = 1.5 s	Time gap = 3 s	Lead vehicle
Fuel consumption [l]	0.84	0.72	0.84
Improvement [%]	0	14	-

Table 4.9: Fuel consumption in RDE urban cycle

The better behaviour of the controller with higher time gap can be seen also by the efficiency map of the motor. In particular the BSFC map (figure 4.15) shows that increasing the time gap the working points area is decreased and it is located at lower torques.

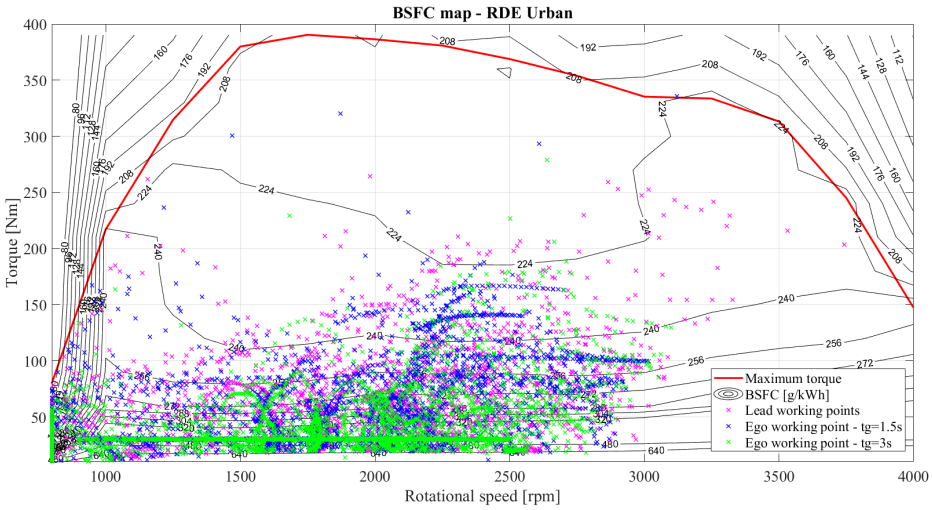

Figure 4.15: BSFC map in RDE urban cycle

RDE rural

The RDE rural driving cycle is characterized by higher speeds and acceleration values. Tests were carried out with different time gaps, and the lowest value that allowed to satisfy the car-following requirements was 4 seconds. Lower time gaps did not respect the safety distance, especially in the deceleration phase, or resulted in an unstable acceleration command, therefore the analysis was carried out considering only

the 4 seconds time gap.
The speed profile for the controller is reported in figure 4.16.

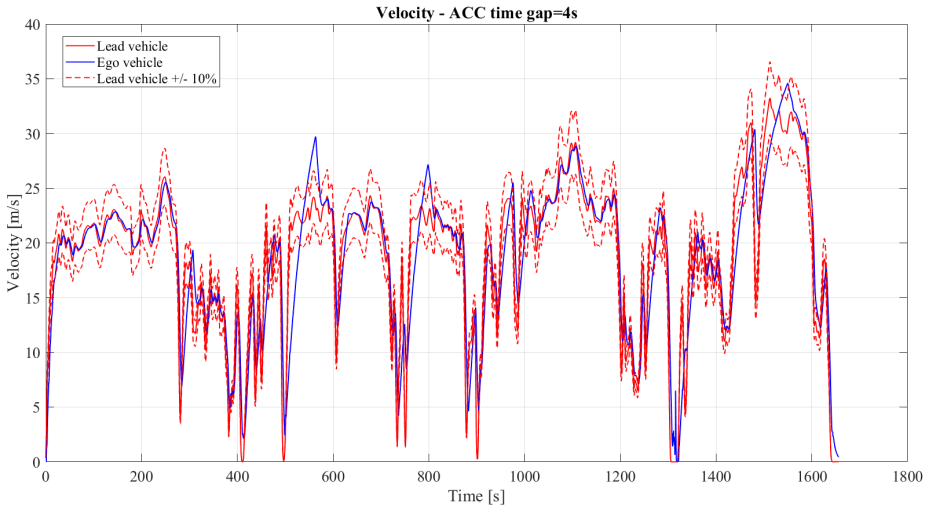

Figure 4.16: Speed profile for RDE rural cycle, time gap = 4 s

The car-following performances are reported in table 4.10. The speed profile is in the desired range for the majority of the time and the covered distance is almost the same, so the requirements can be considered satisfied.

Parameter	Time gap = 4 s	Lead vehicle
Covered distance [km]	31.24	31.23
Maximum deviation [m/s]	14.10	-
Average deviation [m/s]	1.93	-

Table 4.10: Car-following parameters in RDE rural cycle

Also, the relative distance between ego and lead car is within the required thresholds.

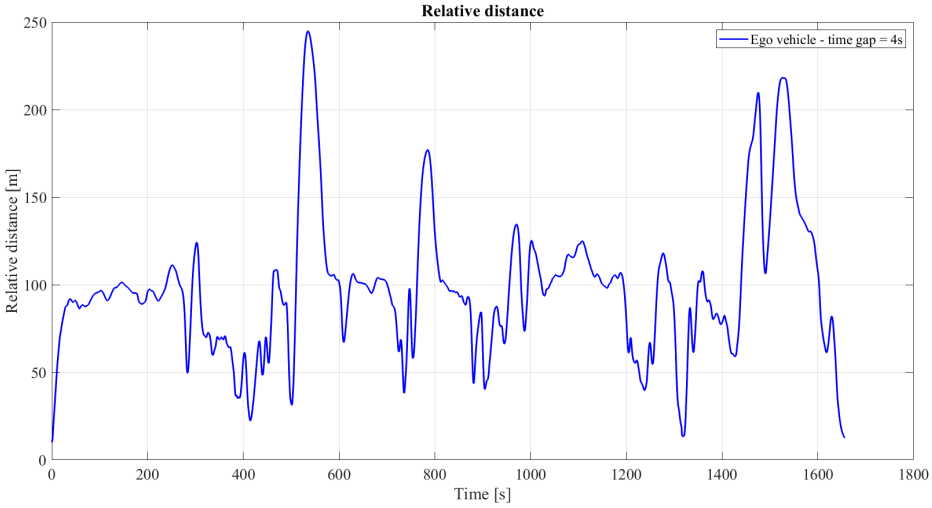

Figure 4.17: Relative distance for RDE rural cycle

The acceleration command is stable and shows a smoother profile with respect to the one of the lead car (figure 4.18).

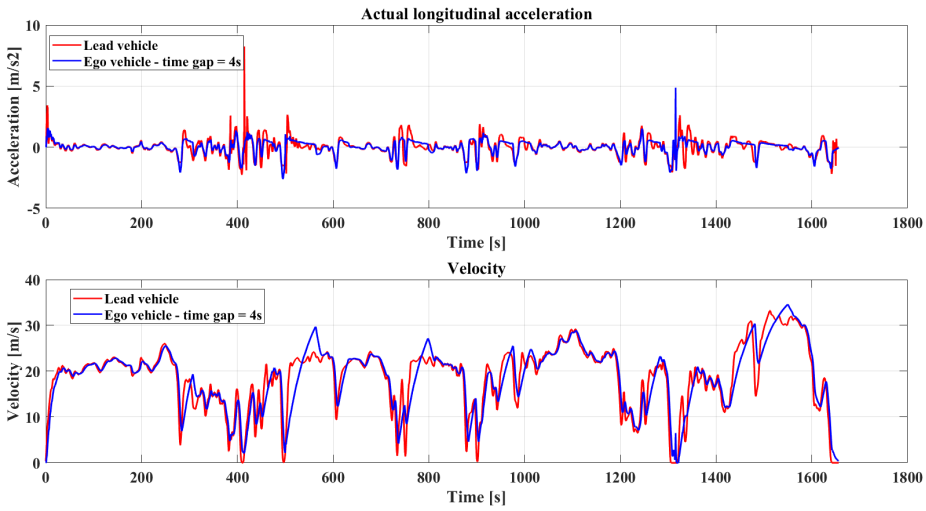

Figure 4.18: Acceleration and speed profile for RDE rural cycle

This results in an improvement in fuel consumption:

	Time gap = 4 s	Lead vehicle
Fuel consumption [l]	3.43	3.63
Improvement [%]	5.5	-

Table 4.11: Fuel consumption in RDE rural cycle

Evaluating the efficiency maps of the motors it is possible to notice that the system equipped with ACC works with lower torque values, improving fuel-economy.

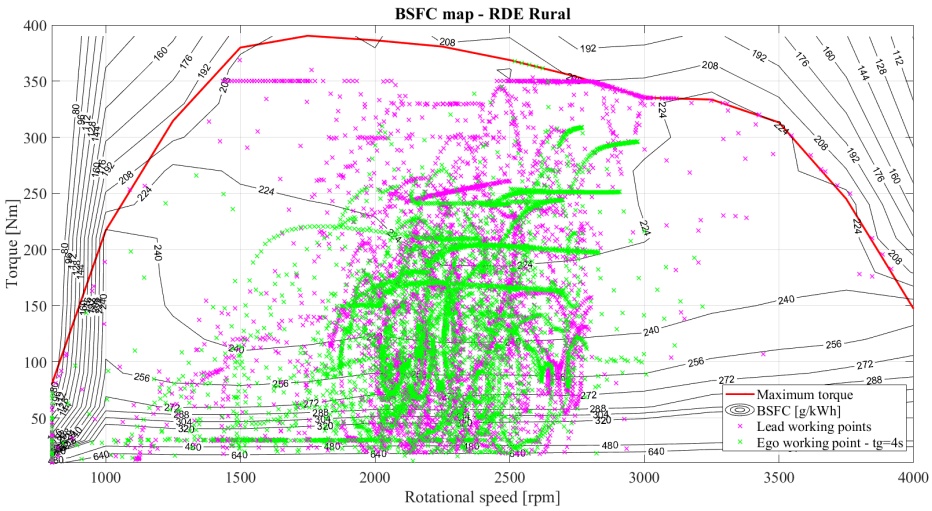

Figure 4.19: BSFC map in RDE rural cycle

RDE motorway

The RDE motorway driving cycle is characterized by high speeds, typical of highways scenarios, and steep accelerations and decelerations. For this reason, low values of time gap could not maintain the safety distance during braking, with the ego car crashing into the lead car. This can be observed in figure 4.20, where the relative distance is negative after 800 seconds. From the tests, it resulted that the minimum time gap that satisfied the requirements is 8 seconds (figure 4.21). The analysis was carried out considering this parameter value.

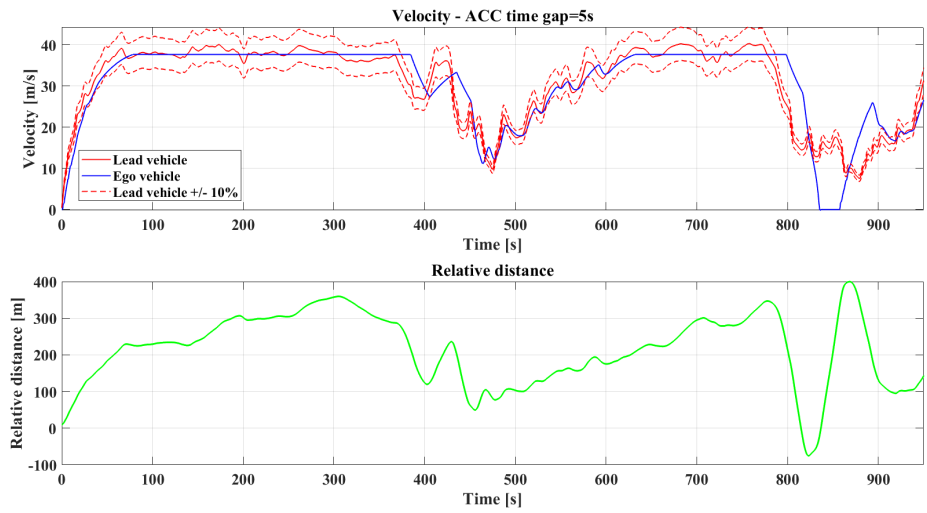

Figure 4.20: Velocity and relative distance in RDE motorway with time gap 5 seconds

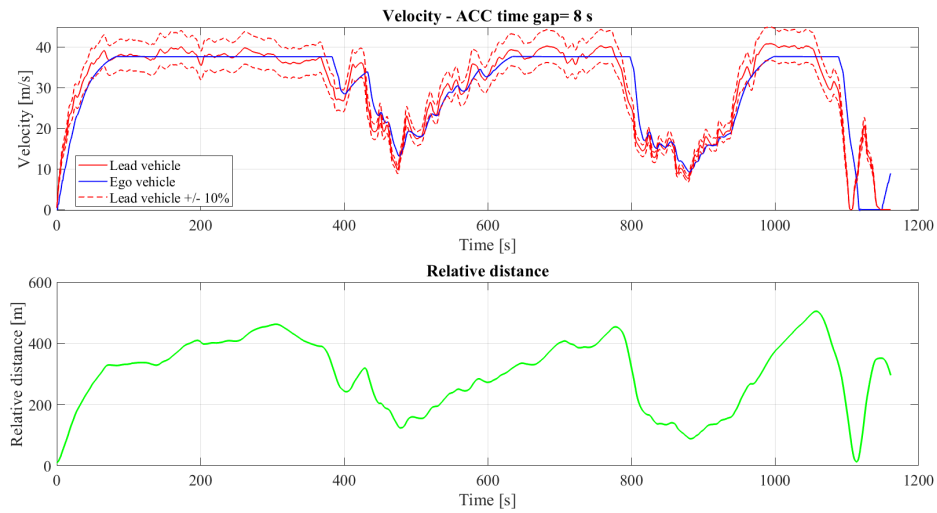

Figure 4.21: Velocity and relative distance in RDE motorway with time gap 8 seconds

The velocity profile at the end of the cycle is outside the desired range, and the acceleration profile is slightly unstable in that interval (figure 4.22), but it is smoother than the lead vehicle's one. However,

higher values of time gap would lead to a relative distance that is not compatible with the upper limit requirements.

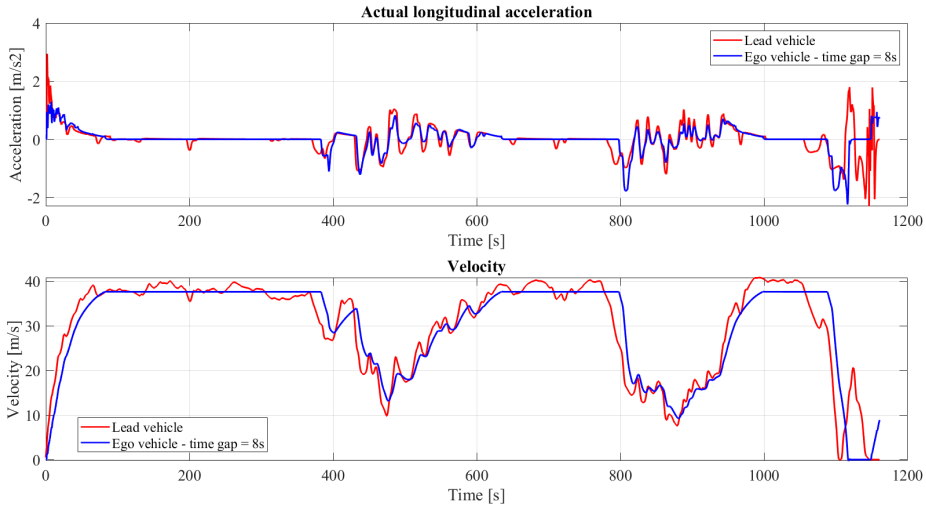

Figure 4.22: Acceleration profile in RDE motorway with time gap 8 seconds

The car-following performances of this controller are reported in the following table:

Parameter	Time gap = 8 s	Lead vehicle
Covered distance [km]	34.7	34.0
Maximum deviation [m/s]	28.8	-
Average deviation [m/s]	3.32	-

Table 4.12: Car-following parameters in RDE motorway cycle

The controller shows a bad performance in terms of fuel consumption.

	Time gap = 8 s	Lead vehicle
Fuel consumption [l]	5.76	5.44
Improvement [%]	-5.8	-

Table 4.13: Fuel consumption in RDE motorway cycle

This can be explained also by looking at the BSFC map of the ICE: a big part of the working points of the system with ACC is located at the maximum torque, which requires higher fuel quantities.

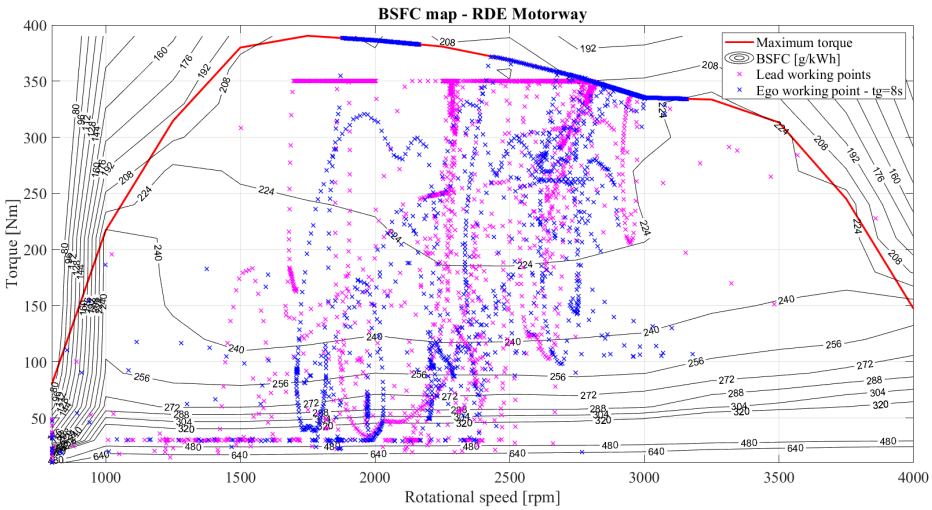

Figure 4.23: BSFC map in RDE motorway cycle

From this analysis it is possible to evince that the considered ACC does not bring any advantages in driving cycles with aggressive profiles, such as the RDE motorway.

US06

The US06 is another driving cycle that represents high speed profiles. Also in this case the tests demonstrated that a higher time gap value is needed to maintain the minimum safety distance and to obtain a stable acceleration command. The lowest acceptable value, as for the RDE

Motorway, is 8 seconds. The relative speed profile and acceleration command are shown in figure 4.24. Lower time gaps led to unstable acceleration commands, in the attempt to satisfy the car-following requirements.

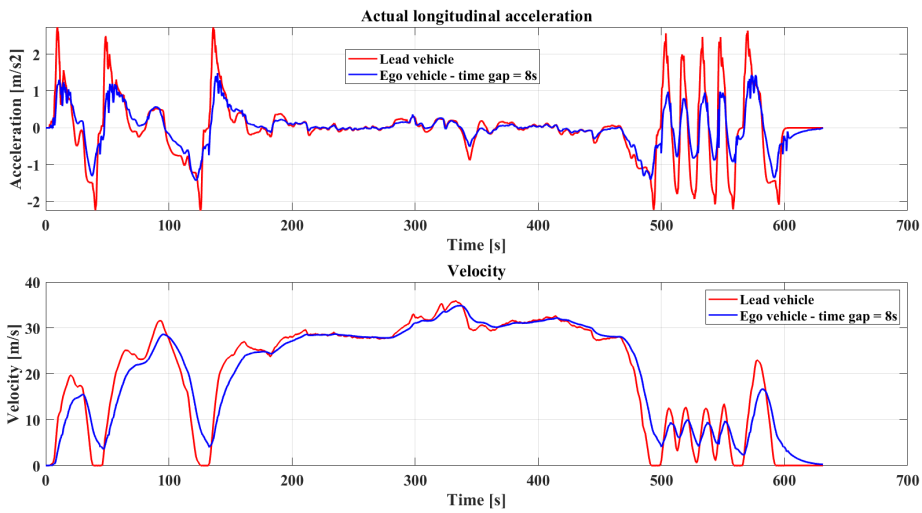

Figure 4.24: Velocity and acceleration in US06 with time gap 8 seconds

The relative distance is between the desired thresholds, and the car-following parameters are satisfied in addition to the stability of the acceleration command.

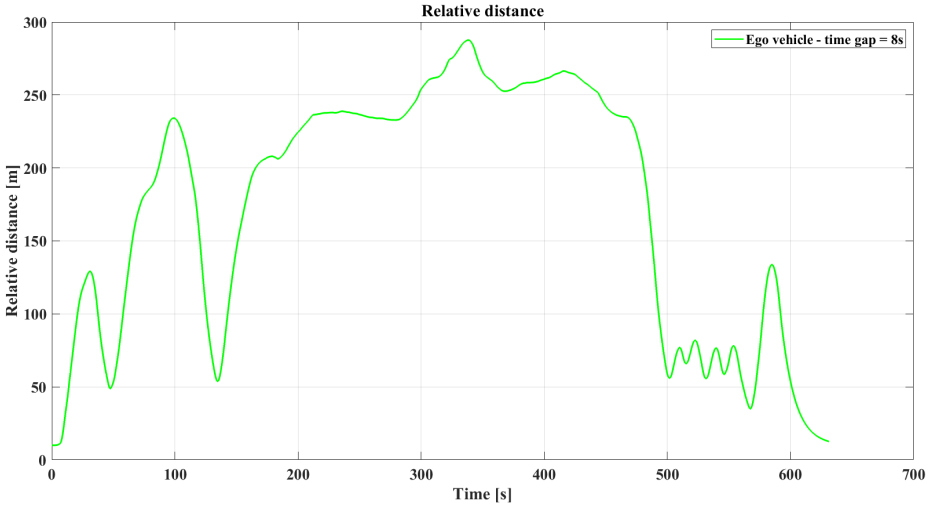

Figure 4.25: Relative distance in US06 with time gap 8 seconds

Parameter	Time gap = 8 s	Lead vehicle
Covered distance [km]	12.9	13.0
Maximum deviation [m/s]	10.2	-
Average deviation [m/s]	2.3	-

Table 4.14: Car-following parameters in US06 cycle

The result is an enhancement of the consumptions:

	Time gap = 8 s	Lead vehicle
Fuel consumption [l]	1.62	1.83
Improvement [%]	11	-

Table 4.15: Fuel consumption in US06 cycle

The motors efficiency maps show that for the ICE in the vehicle with ACC the working points are focused in a more restricted area,

located at lower working torques. This explains the improvement in fuel consumption.

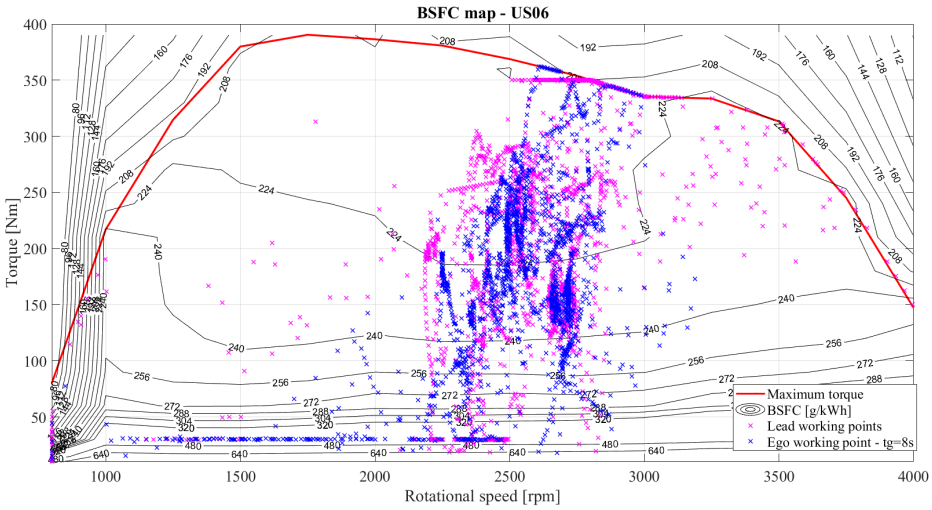

Figure 4.26: BSFC map in US06 cycle

4.3 Integration and test of adaptive-time gap function in Classical ACC

The simulations of the previous section demonstrated that the most suitable time gap value cannot be fixed, but it depends on the driving scenario. Scenarios with higher average speeds, such as RDE Motorway or US06, require higher time gaps, while this value can be softened for less aggressive cycles such as FTP75, WLTC, RDE urban and rural.

Driving cycle	Average speed [m/s]	Time gap [s]
WLTC	13	1.5 - 3
RDE urban	8	1.5 - 3
FTP75	10	3
RDE rural	20	4
US06	22	8
RDE motorway	27	8

Table 4.16: Time gap values for the different driving cycles

For this reason, the Classical ACC algorithm was modified to vary the time gap during a driving cycle, according to the obtained data. The system was integrated with a function that varies the time gap depending on the moving average of the actual velocity of the vehicle. The new function follows this workflow:

1. The function takes as input the actual velocity value of the ego vehicle and stores it in an array.

2. The moving average of the actual velocities array is calculated considering a window of fixed length n of the last n values of speeds.

3. Based on the tuning values of preceding simulations, velocity thresholds for time gap values are established.

4. The function compares the moving average to the thresholds and sets the time gap value.

The new algorithm was tested on the RDE complete cycle, to test its effectiveness on a speed profile that requires different time gaps. The average speed was evaluated in a moving window of 80 seconds. The thresholds are reported in table 4.16.

Threshold [m/s]	Time gap [s]
$v_{avg} < 12$	3
$12 \leq v_{avg} < 24$	5
$v_{avg} \geq 24$	8

Table 4.17: Thresholds for adaptive time gap function

The new speed profile is respecting the car-following requirements also at high speeds, as it is possible to observe from the zoom on the velocity profile in figure 4.28. The speed profile and the time gap command are reported in figure 4.27.

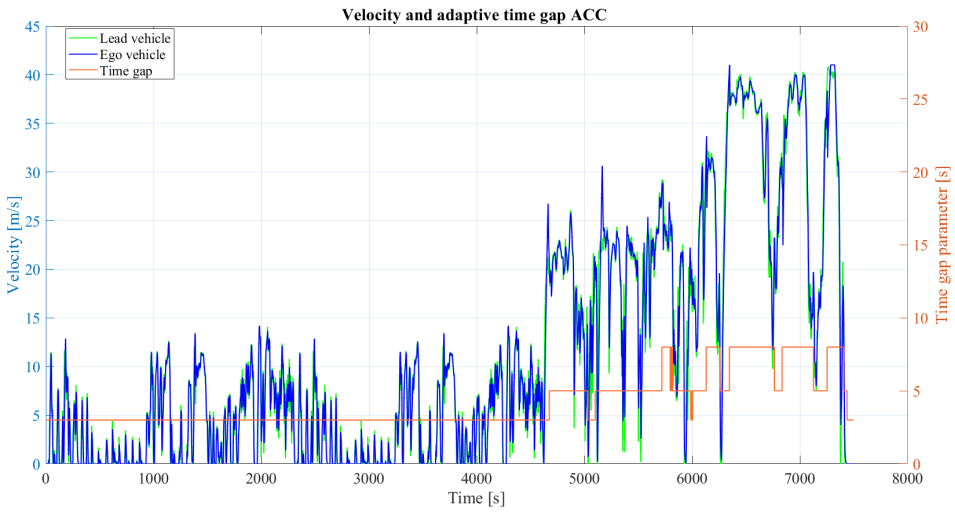

Figure 4.27: Velocity and time gap on RDE complete

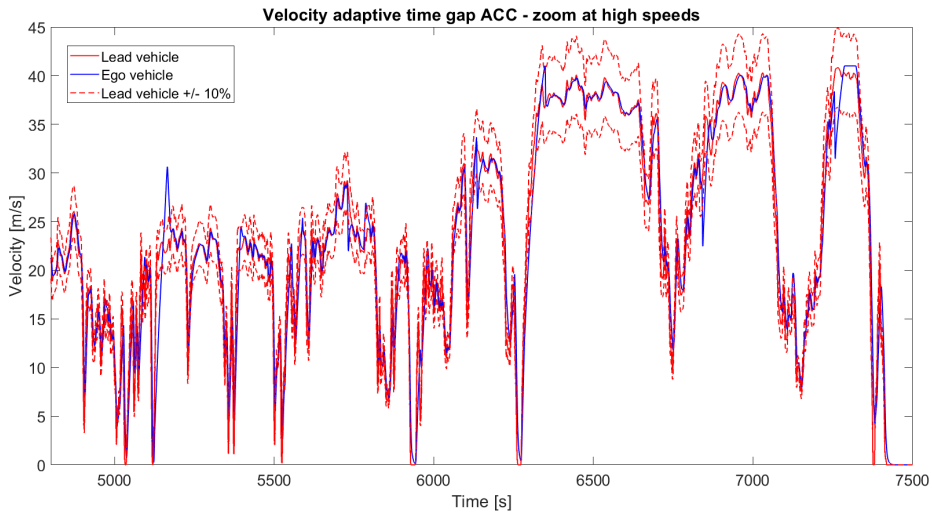

Figure 4.28: Velocity on RDE complete - high speeds

With the adaptive time-gap algorithm, it is possible to ensure that the relative distance is above the minimum safe value through the entire driving cycle, without the need to change the time gap manually. In addition, as it is possible to notice from figure 4.29, the relative distance is lower with respect to the one that is kept by a vehicle with Classical ACC with constant time gap equal to 8 seconds, which is the lowest time-gap that could respect the requirements at high-speed.
The total fuel consumption improvement evaluated is 4.2 %. This improvement is lower with respect to the constant time gap ACC, because in that case the controller is less aggressive and therefore consumptions are lower.

	Adaptive t_g	Constant $t_g = 8s$
Improvement [%]	8.4	4.2

Table 4.18: Fuel consumption improvement with respect to lead vehicle in RDE complete cycle

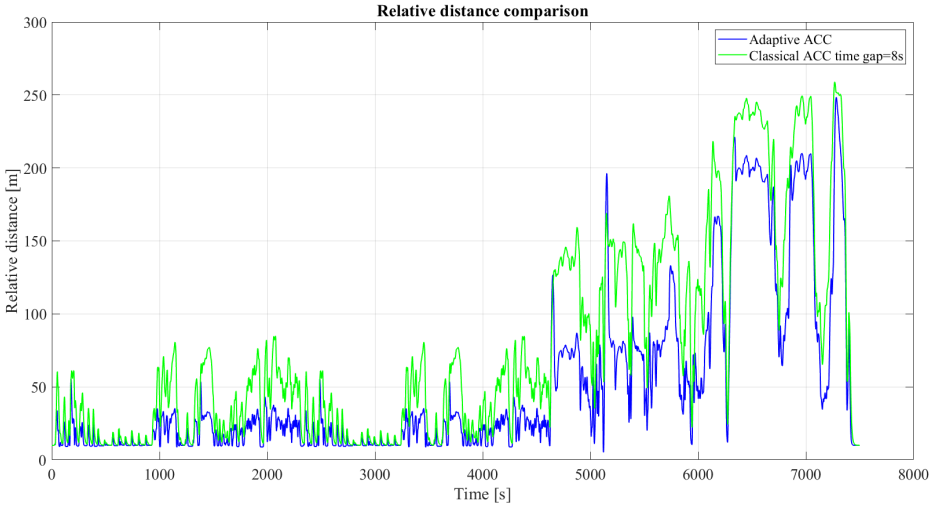

Figure 4.29: Relative distance on RDE complete

Chapter 5

Conclusion

The aim of this thesis work was to optimize the control logic of a Hybrid Electric Vehicle with the introduction of Adaptive Cruise Control, investigating the benefit of such technology in terms of fuel consumption. After tuning the parameters, the results showed that the use of ACC leads to an improvement in the vehicle's performance and efficiency especially at low and medium speeds. It was observed that the ICE was able to work with lower torque requests, and therefore the fuel economy was improved. The percentage of fuel saving depends on the driving cycle used as a reference. However, for high speeds and aggressive driving profiles such as the RDE Motorway, the results were not satisfying and the controller could not lead to a stable and efficient response. In fact, it was not possible to improve fuel economy while respecting the car-following requirements during high decelerations. The torque request could not be managed in an optimizing way by the controller and the ICE was working at high torques and low efficiency for high speeds.
The introduction of an adaptive time gap function allowed the vehicle to travel at a lower relative distance, with better car-following performances and additional benefit on fuel consumption.

Scenario	Average speed [m/s]	Fuel saving [%]
WLTC	13	9.0
RDE Urban	10	14
FTP75	10	5.2
RDE Rural	20	5.5
US06	22	11
RDE Motorway	27	-

Table 5.1: Fuel saving for each cycle with constant time gap ACC

5.1 Future works

Future improvements could focus on the investigation of a new control logic to improve consumptions also in driving cycles that require higher torques. The adaptive time gap function could be developed with the use of predictive strategies such as MPC or neural networks.
A further development could take into account the presence of traffic lights and road signs, and integrate ACC with V2I (Vehicle-To-Infrastructure) communication.
The ACC could be substituted with other ADAS technologies in the high-level controller, to compare the benefits of different technologies on the efficiency of the vehicle.

Bibliography

[1] *Transport and environment report 2021. (Decarbonising road transport — the role of vehicles, fuels and transport demand).* Tech. rep. 02/2022. Luxembourg: Publications Office of the European Union: European Environment Agency, 2022 (cit. on p. 1).

[2] *CO2 emissions from cars: facts and figures (infographics).* 2019. URL: `https://www.europarl.europa.eu/news/en/headlines/society/20190313STO31218/co2-emissions-from-cars-facts-and-figures-infographics` (cit. on p. 2).

[3] *Electric vehicles from life cycle and circular economy perspectives.* Tech. rep. 13/2018. Luxembourg: Publications Office of the European Union: European Environment Agency, 2018 (cit. on p. 2).

[4] *Electric Vehicles.* International Energy Agency. 2019. URL: `https://www.iea.org/energy-system/transport/electric-vehicles` (cit. on p. 2).

[5] National Highway Traffic Safety Administration. «Critical Reasons for Crashes Investigated in the National Motor Vehicle Crash Causation Survey». In: (Mar. 2018) (cit. on p. 3).

[6] SAE International. «Taxonomy and Definitions for Terms Related to Driving Automation Systems for On-Road Motor Vehicles». In: (Apr. 2021) (cit. on p. 3).

[7] Qicheng Xue, Xin Zhang, Teng Teng, Jibao Zhang, Zhiyuan Feng, and Qinyang Lv. «A comprehensive review on classification, energy management strategy, and control algorithm for hybrid electric vehicles». In: *Energies* 13.20 (2020), p. 5355 (cit. on pp. 8, 9, 11).

[8] Ojas M. Govardhan. «Fundamentals and Classification of Hybrid Electric Vehicles». In: *International Journal of Engineering and Techniques* 3 (Sept. 2017) (cit. on p. 11).

[9] *What is the difference between micro, mild, full and plug-in hybrid electric vehicles*. URL: https://x-engineer.org/micro-mild-full-hybrid-electric-vehicle/ (cit. on p. 12).

[10] Onori Simona, Serrao Lorenzo, and Rizzoni Giorgio. *Hybrid Electric Vehicles: Energy Management Strategies*. Springer, 2016 (cit. on pp. 13, 15, 17).

[11] C. Musardo, G. Rizzoni, and B. Staccia. «A-ECMS: An Adaptive Algorithm for Hybrid Electric Vehicle Energy Management». In: (2005), pp. 1816–1823. DOI: 10.1109/CDC.2005.1582424 (cit. on p. 18).

[12] Lina Fu, Ümit Ö zgüner, Pinak Tulpule, and Vincenzo Marano. «Real-time energy management and sensitivity study for hybrid electric vehicles». In: (2011), pp. 2113–2118. DOI: 10.1109/ACC.2011.5991374 (cit. on p. 18).

[13] Bo Gu and Giorgio Rizzoni. «An adaptive algorithm for hybrid electric vehicle energy management based on driving pattern recognition». In: *ASME International Mechanical Engineering Congress and Exposition*. Vol. 47683. 2006, pp. 249–258 (cit. on p. 18).

[14] John T. B. A. Kessels, Michiel W. T. Koot, Paul P. J. van den Bosch, and Daniel B. Kok. «Online Energy Management for Hybrid Electric Vehicles». In: *IEEE Transactions on Vehicular Technology* 57.6 (2008), pp. 3428–3440. DOI: 10.1109/TVT.2008.919988 (cit. on p. 19).

[15] URL: https://it.mathworks.com/discovery/adas.html (cit. on p. 19).

[16] Council of the European Union European Parliament. «Regulation (EU) 2019/2144 of the European Parliament and of the Council». In: (Nov. 2019) (cit. on p. 21).

[17] Olaf Jeroen Gietelink. «Design and Validation of Advanced Driver Assistance Systems». PhD thesis. Netherlands TRAIL Research School, 2007 (cit. on pp. 21, 24).

[18] O. Gietelink, J. Ploeg, B. De Schutter, and M. Verhaegen. «VE-HIL: A Test Facility for Validation of Fault Management Systems for Advanced Driver Assistance Systems». In: *IFAC Proceedings Volumes* 37.22 (2004). IFAC Symposium on Advances in Automotive Control 2004, Salerno, Italy, 19-23 April 2004, pp. 397–402 (cit. on pp. 23, 24).

[19] M. Rimini-Döring, A. Keinath, E. Nodari, A. Toffetti F. Palma, N. Floudas, E. Bekiaris, V. Portouli, and M. Panou. «Aide (Adaptive Integrated Driver-vehicle Interface) considerations on Test Scenarios». In: *Information Society Technologies (IST) programme* (2015) (cit. on p. 25).

[20] *Assisted driving Test & Assessment Protocol - Version 1.0*. Tech. rep. EURO NCAP, 2020 (cit. on pp. 25, 26).

[21] Li-hua LUO, Hong LIU, Ping LI, and Hui WANG. «Model predictive control for adaptive cruise control with multi-objectives: comfort, fuel-economy, safety and car-following». In: *Journal of Zhejiang University-SCIENCE A* (2009) (cit. on p. 25).

[22] Erwin de Gelder, Olaf Op den Camp, and Niels de Boer. *Scenario Categories for the Assessment of Automated Vehicles*. Tech. rep. Centre of Excellence for Testing, Research of Autonomous Vehicles, Nanyang Technological University, Singapore, and the Land Transport Authority of Singapore, Jan. 2020 (cit. on pp. 26, 27).

[23] Emre Kural and Bilin Aksun Güvenç. «Integrated Adaptive Cruise Control for Parallel Hybrid Vehicle Energy Management». In: *IFAC-PapersOnLine* 48.15 (2015), pp. 313–319. ISSN: 2405-8963 (cit. on p. 29).

[24] Andreas Weißmann, Daniel Görges, and Xiaohai Lin. «Energy-Optimal Adaptive Cruise Control based on Model Predictive Control». In: *IFAC-PapersOnLine* 50.1 (2017). 20th IFAC World Congress, pp. 12563–12568 (cit. on pp. 29, 30).

[25] Shengbo Li, Keqiang Li, Rajesh Rajamani, and Jianqiang Wang. «Model Predictive Multi-Objective Vehicular Adaptive Cruise Control». In: *IEEE Transactions on Control Systems Technology* 19.3 (2011), pp. 556–566 (cit. on p. 29).

[26] Yinglong He, Biagio Ciuffo, Quan Zhou, Michail Makridis, Konstantinos Mattas, Ji Li, Ziyang Li, Fuwu Yan, and Hongming Xu. «Adaptive Cruise Control Strategies Implemented on Experimental Vehicles: A Review». In: *IFAC-PapersOnLine* 52.5 (2019), pp. 21–27 (cit. on p. 30).

[27] Mushairry Mustafar, Saiful Anuar Abu Bakar, Z. Zainuddin, Mohd Farris Mansor, N.H.F. Ismail, and M. R. Rani. «Optimal Design of an Adaptive Cruise Control System for Driving Comfort and Fuel Economy». In: *Journal of the Society of Automotive Engineers Malaysia* (2021) (cit. on p. 30).

[28] Changwoo Park and Hyeongcheol Lee. «A Study of Adaptive Cruise Control System to Improve Fuel Efficiency». In: *International Journal of Environmental Pollution and Remediation* (Jan. 2017) (cit. on p. 30).

[29] Yuto Imanishi, Naoyuki Tashiro, Yoichi Iihoshi, and Takashi Okada. «Development of Predictive Powertrain State Switching Control for Eco-Saving ACC». In: *SAE Technical Paper* (Jan. 2017) (cit. on p. 31).

[30] P. Pettersson, B. Jacobson, F. Bruzelius, P. Johannesson, and L. Fast. «Intrinsic differences between backward and forward vehicle simulation models». In: *IFAC-PapersOnLine* 53.2 (2020). 21st IFAC World Congress, pp. 14292–14299 (cit. on p. 33).

[31] Gao Diju, Wei Zhang, Aidi Shen, and Yide Wang. «Parameter Design and Energy Control of the Power Train in a Hybrid Electric Boat». In: *Energies* 10 (July 2017), pp. 1–12. DOI: `10.3390/en10071028` (cit. on p. 42).

[32] URL: `https://it.mathworks.com/help/driving/ug/adaptive-cruise-control-with-sensor-fusion.html` (cit. on p. 45).

[33] Jiří Ambros and M Kyselý. «Free-flow vs car-following speeds: Does the difference matter?» In: *Advances in Transportation Studies* 40 (Nov. 2016), pp. 17–26. DOI: 10.4399/97888548970072 (cit. on p. 49).

[34] Giulia Cilio. «Optimization of the control logic of a hybrid electric vehicle exploiting ADAS information». MA thesis. Politecnico di Torino, 2022-2023 (cit. on pp. 51, 53).

[35] *Generate Drive Cycles for Real Driving Emissions*. URL: https://it.mathworks.com/help/autoblks/ug/generate-drive-cycles-for-real-driving-emissions.html (cit. on p. 54).

[36] *US: LIGHT-DUTY: FTP-75*. URL: https://www.transportpolicy.net/standard/us-light-duty-ftp-75/#:~:text=The%20FTP-75%20and%20the%20FTP72%20are%20two%20variants,after%20the%20engine%20is%20stopped%20for%2010%20minutes. (cit. on p. 55).

[37] *SFTP-US06*. URL: https://dieselnet.com/standards/cycles/ftp_us06.php. (cit. on p. 56).

[38] Luca Nicosia. «Design and validation of a numerical vehicle model for hybrid architectures». MA thesis. Politecnico di Torino, 2022-2023.